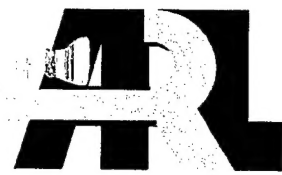


Army Research Laboratory



Search and Target Acquisition: Single Line of Sight Versus Wide Baseline Stereo

By
Wendell R. Watkins

**Survivability/Lethality Analysis Directorate
Information and Electronic Protection Division**

ARL-TR-831

September 2001

20011005 068

Approved for public release; distribution unlimited.

NOTICES

Disclaimers

The findings in this report are not to be construed as an official Department of the Army position, unless so designated by other authorized documents.

Citation of manufacturers' or trade names does not constitute an official endorsement or approval of the use thereof.

REPORT DOCUMENTATION PAGE

*Form Approved
OMB No. 0704-0188*

Public reporting burden for this collection of information is estimated to average 1 hour per response, including the time for reviewing instructions, searching existing data sources, gathering and maintaining the data needed, and completing and viewing the collection information. Send comments regarding this burden estimate or any other aspect of this collection of information, including suggestions for reducing this burden, to Washington Headquarters Services, Directorate for Information Operations and Reports, 1215 Jefferson Davis Highway, Suite 1204, Arlington, VA 22202-4302, and to the Office of Management and Budget, Paperwork Reduction (0704-0188), Washington, DC 20503.

1. AGENCY USE ONLY (Leave blank)	2. REPORT DATE	3. REPORT TYPE AND DATES COVERED	
	September 2001	FINAL	
4. TITLE AND SUBTITLE		5. FUNDING NUMBERS	
Search and Target Acquisition: Single Line of Sight Versus Wide Baseline Stereo			
6. AUTHOR(S) Wendell R. Watkins		8. PERFORMING ORGANIZATION REPORT NUMBER	
7. PERFORMING ORGANIZATION NAME(S) AND ADDRESS(ES) U.S. Army Research Laboratory Survivability/Lethality Analysis Directorate Information & Electronic Protection Division ATTN: AMSRL-SL-EA White Sands Missile Range, NM 88002-5513		ARL-TR-831	
9. SPONSORING/MONITORING AGENCY NAME(S) AND ADDRESS(ES) U.S. Army Research Laboratory 2800 Powder Mill Road Adelphi, MD 20783-1145		10. SPONSORING/MONITORING AGENCY REPORT NUMBER ARL-TR-831	
11. SUPPLEMENTARY NOTES			
12a. DISTRIBUTION/AVAILABILITY STATEMENT Approved for public release; distribution unlimited.		12b. DISTRIBUTION CODE A	
13. ABSTRACT (Maximum 200 words) The purpose of this paper is to present the results of two observer experiments for comparison of the use of wide baseline stereo vision (binocular viewing of two line of sight (LOS) images) and mono vision (binocular viewing of single LOS images) for performing search and target-acquisition tasks. To quantify the advantage of using wide baseline stereo vision, a joint field test was conducted in Soesterberg, The Netherlands in September 1998. A multiple baseline imagery database was obtained with personnel wearing forest camouflage uniforms arrayed at two rural terrain sites. The weather condition for site 1 was clear to partly cloudy and site 2 was overcast with light rain. The preliminary analysis of the site 1 database indicated that wide baseline stereo could be used to improve search and target acquisition but that the baseline was too wide for many of the closer targets at that site. The database from site 2 was then analyzed through observer testing with single LOS and wide baseline stereo displays. The results indicate that stereo vision can be effectively used to reduce false alarm detection rates. Additionally, guidelines for optimum stereo display were obtained that could be used to improve positive target detection.			
14. SUBJECT TERMS search, target acquisition, depth perception, stereo vision, camouflage, clutter		15. NUMBER OF PAGES 83	
		16. PRICE CODE	
17. SECURITY CLASSIFICATION OF REPORT UNCLASSIFIED	18. SECURITY CLASSIFICATION OF THIS PAGE UNCLASSIFIED	19. SECURITY CLASSIFICATION OF ABSTRACT UNCLASSIFIED	20. LIMITATION OF ABSTRACT SAR

Preface

The effects of clutter on search (S) and target acquisition (TA) are of current interest to the U.S. Army Night Vision as well as the North Atlantic Treaty Organization (NATO) working group investigating camouflage, concealment, and deception evaluation techniques. Wendell Watkins of the U.S. Army Research Laboratory (ARL) and Mathee Valeton of the Human Factors Research Institute (TNO) of The Netherlands are members of this NATO working group. Discussions between them in 1998 resulted in an invitation by TNO for Wendell Watkins to perform a joint experiment at TNO under the ARL Professional Exchange Program. The experiment performed was designed to evaluate the benefits of using wide baseline stereo vision over single line of sight (mono) vision. One of the important goals was to show how stereo vision could be used to mitigate the effects of clutter on S and TA, and results indicate that stereo vision can be effectively used to reduce false alarm detection rates.

Acknowledgements

I would especially like to thank Patti Gillespie and the Sensor and Electron Devices Directorate, for without their funding support this research would not have been possible. I am also indebted to Sandor Der for his excellent review of this manuscript. Additionally, I would like to thank Mathee Valeton and the rest of the Vision and Imaging Research Team of The Netherlands Organization for Applied Scientific Research, Human Factors Research Institute, Soesterberg, The Netherlands. Without their assistance in assembling the equipment, processing the photographic slides, and in providing the targets and test range needed for this experiment, this research would likewise not have been possible. The personnel who served as targets will especially remember tromping through heather while getting soaked by rain and trying to guess how to respond to unintelligible hand-held radio messages. I would also like to thank Richard Anaya for his assistance in collecting the observer test data.

Contents

Preface	iii
Acknowledgement	v
Executive Summary	vii
1. Introduction	1
2. Field Experiments	3
2.1 Rationale for Target and Site Selection.....	3
2.2 Site 1 and Site 2 Measurements.....	4
3. Laboratory Tests	5
3.1 Site 1 Presentation Preparation	5
3.2 Site 1 Image Display.....	6
3.3 Site 1 Results.....	6
3.4 Site 2 Test Design	8
3.5 Site 2 Image Display.....	11
4. Observer Database	13
4.1 S and TA Task.....	13
4.2 Target Identifications	14
5. Results	15
5.1 Database Suitability.....	16
5.2 Observer Preference.....	16
5.3 Observer Score.....	17
5.4 Effects of Range and FOV.....	18
5.5 Clutter Rejection.....	22

Conclusions	27
References	29
Acronyms	31
Distribution	65
Appendix.	
Search and Target Acquisition: Single Line of Sight Versus Wide Baseline Stereo Figures and Tables.....	33
Table.	
Average search time for nontargeted/targeted sectors	7

Executive Summary

As the sensitivity and resolution of imaging systems have improved, the targets for which they were intended to detect continue to become less conspicuous. This issue was taken up by the North Atlantic Treaty Organization in the Camouflage, Concealment, and Deception Evaluation Techniques working group. This group's research results showed that addressing concerns such as camouflage design requires a better understanding of search (S) and target acquisition (TA).

One possible means of improving S and TA and clutter rejection may be through the use of stereoscopic vision. However, the ability of stereoscopic vision to make targets "pop out" of scenes has not yet been exploited because of the cost of dual-detection systems. Fortunately, the cost of these systems is dropping, and at the same time, the advantages may offset additional costs.

An S and TA test was conducted that provided single (mono)- and wide baseline stereo imagery for observer testing. The database developed for observer testing contained the same scene with and without camouflaged, human targets present. The analysis results of imagery from the second of two sites have provided valuable findings. Analysis of variance did not show significant differences between single line of sight and stereo vision in general; however, there were differences in the observer responses:

- There was a significant difference in the false target detections (between mono and stereo vision) for the narrow field of view (FOV) cases.
- Analysis of target range effect showed that there was better performance for the small, narrow baseline FOV case with longer ranges.
- Also, there were several targets that could be identified as distribution outliers and rationale for the poorer performance of the stereo vision related to biased displays that favored the mono vision.
- There was only a little difference in total number of correctly detected targets. Nonetheless, this research suggests that about a 20 percent increase in correctly identified targets using stereo vision may be possible to obtain if proper training in the use of stereo vision is given prior to testing and optimized displays are used.

- It appears that as the FOV was decreased from medium to small, mono vision results showed an increase in false alarms, possibly from the effects of global clutter.
- About one-half of the observers showed a substantial decrease in false alarms, indicating again that with proper training in the use of stereo vision and optimized displays, the number of false alarms may be decreased by a factor of 2 using stereo vision.
- Finally, data were obtained that can be used to optimize the display for observer performance using stereo vision.

1. Introduction

Recently there have been some spectacular applications of stereoscopic (stereo) vision. For example, stereo vision was used on the Mars Lander for navigating on the planet surface. It was also used to perform the complex underwater exploration of the Titanic. Most animals have developed stereo vision through evolution. Although a significant portion of the human brain is devoted to deriving motion and depth cues through complex processing of the imagery from both of our eyes, stereo vision is not being widely utilized. One of the reasons for this is that poorly displayed stereo images or video can produce severe eyestrain. At the same time, some positive comparisons showing the benefits of using stereo over mono vision have been made. [1,2] Efforts to better understand and model the complex brain process used to derive the 3-dimensional (3-D) content of the scenes that our two eyes use for stereo have become quite sophisticated and continue to evolve (including the effects introduced by the display system). [3,4,5] Despite these efforts, the use of stereo vision still has not been fully exploited. *Practical Handbook on Image Processing for Scientific Applications* was published recently in which only a dozen pages out of almost 600 are devoted to stereo vision applications. [6] The recent improvements in heads-up and head-mounted displays may open the door for more widespread use of stereo vision especially since the utility of sophisticated 3-D scene modeling is enhanced by the use of stereoscopic displays. There is one area that has not been addressed, and that is the use of wide baseline stereo vision for search (S) and target acquisition (TA). [7]

The rationale for performing the research presented in this paper is derived from the test results from the Distributed Interactive Systems Search & Target Acquisition Fidelity (DISSTAF) conducted at Fort Hunter-Liggett, CA in 1995. The visible data sets collected by the Dutch are currently being used to evaluate the camouflage, concealment, and deception performance models for the NATO SCI-12 Working Group. [8] A group from the U.S. Army Research Laboratory (ARL) collected wide baseline stereo imagery at the DISSTAF Test. The results of showing this stereo imagery to some of the observers used for the DISSTAF Test was that there are depth cues that can be used at multiple kilometer ranges for S and TA tasks. These results, coupled with the application of stereo vision for detecting camouflage, need to be quantified for comparison with the biocular single line of sight (LOS) (mono vision) S and TA methodology. [9] The problem is

that there are currently no good models for handling clutter in imagery, even for single LOS imagery analysis, especially when the targets are camouflaged. This deficiency was recently highlighted by James Ratches of the U.S. Night Vision at the SPIE AeroSense Symposium in an Invited Overview paper of Night Vision's efforts past, present, and future. [10] Notably, clutter quantification was on the top of the list for future research.

2. Field Experiments

An S and TA test was performed under an exchange scientist program with the Netherlands Organization for Applied Scientific Research (TNO), Human Factors Research Institute at Soesterberg, The Netherlands, in September 1998. The test was performed at a military training base, using four scientists from TNO wearing Dutch forest camouflage uniforms as participants. Sets of wide baseline stereo photos were obtained for targeted and nontargeted/targeted scenes at two sites. The targeted and nontargeted scene photographic slides were taken on the same day within a few minutes of each other. The imagery obtained was taken with 35-mm cameras with 200-mm lenses for target ranges from 100 to 900 m. A single field of view (FOV) was used for all of the targeted and nontargeted scenes at each site. The photos were taken with color slide film and were digitized to 3 x 2 K pixel resolution. The imagery data sets were used to perform S and TA tests.

2.1 Rationale for Target and Site Selection

There is no standard method for comparing mono versus stereo vision for various S and TA tasks. Hence, the targets were positioned with the objective of quantifying the impact of scene clutter on S and TA for both mono and stereo LOSs. The simplest targets to use were humans with camouflaged attire to sufficiently match the surroundings so that the targets were not obvious and sufficient clutter was present to assess target placement in different clutter regions. The assessment imagery database also had to have several LOSs for stereo vision for comparison with mono vision performance for the same task. The human interocular separation for maximum unaided depth perception ranges is about 10 mrad. Multiples of this separation was utilized for assessing the performance of stereo versus mono vision for the same S and TA task.

With a 35-mm camera, a camouflaged human can only be detected in digitized photographic film slides to a range of about 300 m. Therefore, 200-mm lenses were used that yielded an FOV of 15 x 10. Each camera's LOS was positioned with a conspicuous feature in the center of the FOV. There were 24 total target locations identified for each of the two sites that represented easy to difficult targets for detection. These locations were referenced to several prominent scene features that were ranged with a binocular range finder.

2.2 Site 1 and Site 2 Measurements

Sufficient 35-mm cameras and 200-mm lenses were obtained to set up four stereo cameras. The targets used were humans wearing Dutch forest camouflage uniforms shown in appendix figure A-1. The test was conducted over a 2-day period at the Soesterberg Artillery Facility where two sites were used.

1. Site 1 had shorter ranges (110 to 675 m) with sunny and partly cloudy conditions.
2. Site 2 had longer ranges (400 to 900 m) with cloudy/rainy conditions.

Site 1 had four camera positions with 6-m separation, and the second had three camera positions with 10-m separation (as shown in appendix figure A-2). Targets were arrayed in each of six different target locations. Slide photos of designated target positions, targeted scenes, and nontargeted scenes were taken at each of two test sites. The result was an imagery database with 24 targets for four stereo LOSs for site 1 and three stereo LOSs for site 2. Because photos were taken with and without the targets present, it is possible to analyze the impact of target placement and background clutter levels.

The targets were positioned in six different locations with overall target ranges from approximately 110 to 660 m for site 1 and 400 to 900 m for site 2. The cameras were placed on tripod mounts in a straight line (perpendicular to the LOS) to the middle of the target-scene FOV, about 1.5 m above the ground. When the four targets were in their first position, the LOS from each of the stereo cameras to each target had to be checked to ensure that the LOS was not blocked. Then, the targets held up large white cards to designate their position, and one photographic slide was taken as quickly as possible from each of the stereo cameras. The targets were then instructed to turn around and hide their card and take either standing or crouching positions. By facing away, the targets did not expose face or hand features that are strong detection cues for visible images. Two slide photos were taken of these targeted scenes from each of the stereo cameras. Then the targets were instructed to hide, and two slide photos were taken of these nontargeted scenes. The 24-target positions were obtained by repeating this process six times. The target scene for site 1 without targets is shown in appendix figure A-3. A composite target scene for site 1 with all 24 targets with their white signs is shown in appendix figure A-4. The corresponding scenes for site 2 are shown in appendix figures A-5 and A-6. Note that only 23 out of 24 targets could be found in site 2.

3. Laboratory Tests

A cursory examination of the two testing sites (shown in appendix figures A-3 through A-6) indicated that it was much easier to locate the targets for site 1. Therefore, the initial data analysis necessary for producing an imagery presentation for observer testing was performed on the site 1 images.

3.1 Site 1 Presentation Preparation

Appendix figure A-4 shows the location of the 24 target positions from the far right camera (of the four cameras with baseline separations of 6 m between each one). The targets are confined to just over one-half of the vertical extent of the whole 3072 x 2048 pixel-digitized image. The initial approach was to place a rectangular grid over the picture to isolate the targets in separate, rectangular sectors so that the targets were not divided into multiple sectors. This result was obtained with only minor target clipping by using a rectangular array of 7 sectors wide x 4 sectors high with each sector being 396 pixels wide x 264 pixels high. *Adobe® Photoshop®* software was used to splice together some of these sectors from the large images containing the targets because not all of the targets in the resulting multiple-targeted sectors were present at the same time. The array was labeled as shown in appendix table A-1 with each sector representing a $1.9^\circ \times 1.3^\circ$ FOV. There were 9 sectors with no targets, 15 sectors with 1 target, 3 sectors with 2 targets, and 1 sector with 3 targets. This set of 28 small FOVs represented the target scenes whether or not a target was present. The same grid was used on the large digitized image with no targets present to produce a set of 28 small, nontargeted FOVs. Because the observer task intended to investigate clutter in the form of false targets, the sector scenes contained an unrestricted number of targets. The observers' task was to determine if there were none, one, or more than one target in each scene.

3.2 Site 1 Image Display

Computer monitor displays were the only means available to observers. *Adobe® Photoshop®* was used to produce sets of targeted and nontargeted sector .bmp files of 792 x 528 pixels or 1.2 Mbytes for the RGB-color image from the original 396 x 264 pixel images. There were 56 total images for the right LOS. In order to obtain the correct stereo image for the other LOSs, the center terrain feature of the right LOS was found in the other LOS whole-scene images and a 396 x 264 rectangular-image sector was cut out around this center feature. As the angular separation increased, there were a few sectors that could not be matched. A random ordering of the targeted and nontargeted sectors was performed such that the ranges' targeted and nontargeted images were randomly mixed with the constraint that the same sector targeted and nontargeted scenes were separated by several intervening different sector images. Finally, because of the limited number of sectors, targeted sector A4, which had an easily detected target, was shown first as a learning image. *Microsoft® PowerPoint®* was used to produce four separate slide shows of 128 scenes. The targeted and nontargeted scenes were each separated by a numbered scene with a black background. The first scene in the slide show was one of the numbered scenes with black backgrounds.

3.3 Site 1 Results

Because the results of site 1 testing impacted how site 2 test was designed, it is necessary to synopsize the results of site 1 observer. Detailed results are given in "Depth Perception Applied to Search and Target Acquisition." [11] When the observers were shown the slide presentation, the location of the real and false target detections were recorded as well as the search time for each sector presented. In further discussion, the observers were shown only the right LOS images on a single-monitor display.

In general, the search times for the nontarget sectors are longer than for the target sectors. In fact, there were only two cases where the target sectors had longer times than the overall average search time of 6.25 s. Longer times in these sectors are logical for they are the most difficult sectors in which to find targets (see the table (next page) for the average search time). [11]

Table. Average search time for nontargeted/targeted sectors

Average search time		
	Nontargeted sectors	Targeted sectors
Low difficulty	-	4.0 s
Medium difficulty	6.7 s	7.5 s
High difficulty	7.5 s	-

The range of average search times for individual observers was from 1.75 to 13.88 s. There was a correlation between poor overall scores and longer search times. To better compare the results of the different observers with respect to the differences between times taken to search individual sectors, the search times of each observer were divided by that observer's average search time to obtain normalized search times. When this was done, there were 852 sectors where no target or a false target was detected taking an average normalized time of 1.15. There were 828 sectors where targets or false targets were found taking an average normalized time of 0.81. In general, it also took longer to determine that there was no target or a false target present than when there was. When the false targets present were very target-like, as in the case for most of the medium difficulty nontargeted sectors, the detection time was short and the nondetection time was long. In sectors where most of the observers found no targets, the search times increased, and when detection was made, it was a false target (this is similar to over training a neural net).

This research provided a few examples of how moderate to difficult targets are missed in scenes when there is an easier target or false target detected first. Specifically, sector B4 had three targets present with positive identification (ID) difficulties of low, medium, and high located, in the left center, right center, and center of the sector, respectively. This image provided a good example of how the human-detection process works: When a S and TA task is given, a fuzzy notion is formulated of what the target of interest is. The scenes are searched for the fuzzy target. If a detection of a real or false target is made, the target construct becomes well-defined and the scene search is rapidly completed thereafter even if multiple targets are present and detected. This refinement in the target sought can cause targets to be missed. In this particular sector, there is a fairly easy standing target to detect right in the middle. The crouching target to the left and away from the tree line was detected only when it was seen first; only 2 of the 30 observers accomplished this. Both of these observers

were able to then detect the easy standing target in the center, but did not detect the medium difficulty standing target in the right center. A similar occurrence happened in sector A1, where there was a bush that very much resembled a standing target in the center of the sector. This made the detection of the crouching real target in the bottom center more difficult.

Finally, an initial attempt at presenting the stereo slide shows to observers revealed some distinct problems. The observers found that the images in the closest sectors could not be fused for the FOV of the entire sector—there simply was too much parallax. At 110 m, the approximate 1.9-m high human targets represent about 90 percent of the sector image height (238 pixels). At 650 m, the human targets represent only about 15 percent of the sector image height (40 pixels). With a 6-m platform separation between the right and right center cameras, the resulting shift between the bottom and top elements of the scenes in the D sector is 1.8 m (225 pixels) with the standing target experiencing 90 percent of this shift from bottom to top. In the C sector, the parallax shift bottom to top is 5.0 m (180 pixels). This time a 1.9 m target in the bottom of the scene would represent only 45 percent of the height with only about 81-pixel parallax shift from the bottom to top of the target. Stereo fusion at this range was possible but not comfortable. Finally, in the B sector the parallax shift bottom to top is 6.3 m or 145 pixels. Now, the 1.9-m target in the bottom of the scene represents just 25 percent of the height with only about 36-pixel parallax shift from the bottom to top of the target. These images could be fused easily and showed good depth perception. Hence, to be able to compare the results of mono to stereo vision for the near targets would require a display of an FOV about one-third the one that was used for the closest sectors.

3.4 Site 2 Test Design

The main purpose of the observer test was to address the question of which viewing condition (mono or stereo) gives the best S and TA results. Several lessons were learned from the observer test on site 1 data even though the *Microsoft® PowerPoint®* presentations produced in stereo could not be used. Using the stereo imagery displays from site 1 with the 6-m baseline and the FOV chosen, only the images with ranges of 300 m or more could be readily fused. Hence, for the same FOV images for site 2 with 10-m baseline, the ranges 500 m and larger should be easily fused. But the impact of FOV on S and TA was not known; therefore, the three following FOVs were used: (1) One very close to the one used for site 1 observer test (384 x 240 pixels instead of 396 x 264 pixels), (2) one 50 percent larger, and (3) one 50 percent smaller.

This matched the standard *Adobe® Photoshop®* gridline block sizes of 24 x 24 pixels as summarized in appendix table A-2. Also, the impact of baseline separation was not known. Hence, for the smaller FOVs both 10 m and 20 m baseline separations were used.

The imagery from the second day's testing at site 2 was collected with three different cameras. Of the three camera positions, the photos from the left camera had the best image quality. The center and right camera photos were a little blurrier, and all three had slightly different color composition even though all the cameras were set to the same exposure and aperture settings. The 200-m lenses must have had optics with different color transmission. These differences did not cause as much of a problem as with site 1 image processing of the stereo image pairs with *Adobe® Photoshop®* because the overcast light rain conditions tended to mute the color differences somewhat. To begin, the left LOS was used as the reference. A composite picture of all of the target locations (see appendix figure A-6) was produced by splicing the target photos with white location cards displayed onto the photo with the first four target positions.

Observer testing was approached as was the testing performed for site 1 imagery database. Instead of reducing the number of available scenes by placing only one target in each scene, both single and multiple targeted scenes were included in the test. Even so, the terrain in the imagery scene (as shown in appendix figures A-5 and A-6) only allowed a limited number of targeted scenes of medium and large size to be extracted for the observer tests. There were two targets (one in the bottom center at 236 m and one to the left of the bunker along the bottom center road at 335 m) that were too close for the entire image to be easily fused in stereo with the large or medium FOV images. Nevertheless, the target next to the bunker was included in a large FOV scene and both were included in medium FOV scenes.

The medium FOV-scene size was chosen as 384 x 240 pixels to closely match the 396 x 264 pixel sectors used in the observer test for site 1. The size was chosen for ease in processing the different FOVs using *Adobe® Photoshop®*, since the standard overlay gridline blocks are 24 x 24 pixels. Therefore, the medium FOV is 16 blocks wide x 10 blocks high. This selection made it easy to get the 50 percent larger and smaller FOVs. The large FOV is 24 x 15 blocks and the small FOV is 8 x 5 blocks.

By selecting various positions for the different FOV templates in the overall scene, a distribution with different numbers of targets was obtained. There were between one and three targets in the large FOV, one and five in the medium FOV, and one or two in

the small FOV. Because there were only a limited number of large and medium FOVs, they were combined into one *Microsoft® PowerPoint®* presentation, and the small FOV images were put into a second presentation. There were only 23 total targets because one could not be found (only three white cards were visible in one of the six target locating scenes). There were 10 large FOV scenes selected with 22 of the 23 targets included. There were 12 medium FOV scenes selected with all 23 targets present. These sets were divided into two groupings of 5 large and 6 medium scenes that contained 22 or 23 nonduplicated target locations. To these 2 sets, 11 scenes were added that represented the nontargeted scenes that were used in the other group. Hence, each group contained the same total of 22 scenes but only one-half of them had targets. From site 1 imagery, five scenes were selected for which good stereo pairs could be produced. These were added to the beginning of both sets as training scenes. The small FOV presentation contained 20 targeted scenes and the same 20 nontargeted scenes but with no target/nontarget pair in close proximity.

Next the issue of wide and narrow baseline separation was addressed. The large and medium FOV presentation used only the 10-m baseline stereo. The small FOV scenes were divided into 2 groupings of 10 with 11 or 12 targets in each group. One group was displayed with 10-m baseline stereo and the other with 20-m baseline stereo. The targeted scenes shown within these two groups with one baseline had their corresponding nontargeted scenes shown with the other baseline. Then two separate presentations were made up of both the large/medium and the small FOVs with targeted and nontargeted scenes reversed. A second random ordering of these sets were made and two more flip-flopped target/nontarget presentations were again made. Hence, there were a total of four each of the two types of FOV presentations. Examples of the three different FOVs and the level of difficulty of target detection are shown in appendix figures A-7 through A-10.

The level of difficulty of the targets was quite good compared to site 1 scenes. One of the problems as mentioned above with site 1 targets was that they were too easy to pick out. In fact, 80 percent of the targets were correctly identified by 90 percent of the observers as shown in appendix table A-3. Nonetheless, five of the longer range A and B sector scenes from site 1 were effectively used to train the observers on both the single LOS and stereo vision S and TA task (as shown in appendix figures A-11 through A-15).

3.5 Site 2 Image Display

In order to present the images to the observers, two separate computers were used with their monitor displays side by side. The person running the test could use cross-eyed stereo viewing of the monitor displays to interpret the results given by the observer. The monitor displays were converted to video by two TView Gold® signal converters and displayed by a modified pair of Virtual IO stereo goggles that allowed the left and right displays to be driven by different video signal inputs. For mono vision, the same left *Microsoft® PowerPoint®* presentation was displayed by both computers. For stereo vision, the left view *Microsoft® PowerPoint* presentation was fed into the left goggle display and the other *Microsoft® PowerPoint®* presentation (center and right LOS) was fed into the right goggle display. The target scenes were separated by a black-numbered scene that allowed the viewer to retain a dark-adapted state during the course of the experiment. The room lights were kept low to provide a noninterfering light level for optimum use of the stereo goggles.

4. Observer Database

Because the focus of this paper is to compare stereo vision and mono vision for S and TA tasks, only the database from the site 2 test will be considered here. There were a total of 36 observers that took two stereo vision tests and two mono vision tests. One test included 22 or 23 targets positioned in large and medium FOV scenes. The other test included 23 targets positioned in small FOV scenes with the stereo portion displayed with either 10-m or 20-m camera baseline separation.

4.1 S and TA Task

Some of the most useful S and TA information can be obtained using eye tracking of the observer. Unfortunately, this type of analysis tool was not available. Hence, an S and TA task was given with an associated rating system to obtain the desired type of response. The observers were split into two groups with one group performing the mono test first and then the stereo 2 weeks later. The second group took the stereo test first and the mono test 2 weeks later. The general task was given as follows for both tests with the stereo portion only given when that test was taken.

- General task instructions—Your task is to find all of the forest-camouflaged personnel targets standing or squatting in the scenes as quickly as possible. There may be one, none, or more than one target in each scene. Once all targets have been located you are to say “stop.” Then tell how many targets were found and their location T-L (top left), T-C, T-R, C-L, C, C-R, B-L, B-C, or B-R; your search will be timed. For the purpose of detection accuracy, 2 points will be added for every target correctly identified, 3 points will be subtracted for every missed target, and 1 point will be subtracted for every false target identified (i.e., $SCORE = 2 \times [Positive\ ID] - 3 \times [Missed\ Targets] - 1 \times [False\ Alarms]$). The targets are not trying to hide and expose only a small portion of their bodies, but the difficulty in identifying them will range from obvious to very difficult. The testing conditions were overcast with light rain.

- Stereo test—For the stereo testing portion of the test the observers were shown an example of what scene fusion meant as illustrated by appendix figure A-16. The observers were then trained on the use of this fusion technique to isolate different range portions of the training scenes from site 1. For both portions of the test (mono and stereo) the observers were told that the concept was to determine which of the two techniques worked better for the S and TA task and that both should be approached with the same criteria. They were told that they would lose more points for missing a target (3 points) than they would get if they correctly identified a target (2 points) and that they would lose only 1 point for a false target. The rationale was to get them to make educated guesses to assess the impact of clutter on the S and TA process. Additionally, after both tests were taken and before they were told how well they performed on either test, they were asked to distribute 5 points between the 2 approaches. The more points assigned meant the better they liked that particular mode of scene presentation.

4.2 Target Identifications

The observers were screened by participating in a stereoscopic visual acuity test to determine if they could see in stereo and how well. [12] A testing schedule was set up to ensure they could take both tests 2 weeks apart. The observers were presented the *PowerPoint®* slide show after they had become dark-adapted to the room lighting. They were shown the five training slides first. Then, they were shown a black-background slide with a number on it; this slide was easily stereo fused. They were then timed as they searched the test scene for targets. When they said, "stop" the watch was stopped and the time recorded. They then told the number and location of the targets found. The person running the test was viewing the same scene on the computer monitors and would determine whether there was a possible ambiguity in correctly identifying real targets. If there was any question, the scene was revisited and the computer arrow of the observer's dominant eye was used to point out the exact location where the target in question was located to determine if a positive ID was made.

5. Results

An analysis of the variance (ANOVA) was performed on the observation data collected at the U.S. Military Academy (USMA), West Point. Copies of the score sheets were used to build a database in the USMA's Minitab 13 statistical software with 4608 data entries or 7 variables for each observer. These included mono or stereo vision; large, medium, or small FOV; and narrow or wide stereo baseline. There were also several nuisance variables that included gender, test order, and visual acuity. The detailed analysis performed is located in "A Comparison of Observer Task Performance: Three Dimensional Versus Two Dimensional Displays." [13] Therefore, this report will provide an overview of the findings rather than the complete, detailed analysis.

First, some of the nuisance factors showed statistical significance: males did better than females. Visual acuity was also significant with the 30 and 60 mrad visual-acuity observers performing better. Also, the order results were different, but not statistically significant. It appears that the observers learned how to better discriminate the false targets when they saw the stereo first and, hence, did better on the mono portion of the test than those observers that took the mono test first. The analysis of the mono versus stereo vision showed a difference, but it was not statistically significant. The analysis of the FOVs showed statistical significance and the results were better with the small FOV. Finally, the analysis of the baselines showed that the 10-m baseline outperformed the 20-m baseline and the mono vision, but did not reach statistical significance. Based on these results, two main issues require further investigation:

- How are the stereo vision results different than the mono vision?
- And what are the requirements for optimizing the stereo vision display?

5.1 Database Suitability

The analysis will begin with the suitability of the target-detection difficulty of site 2 scenes. This is summarized in the appendix tables A-4 and A-5. The difficulty level is divided into three equal categories for each FOV. The top third is listed as easy (E), the middle as (M), and the bottom as hard (H). The cutoff point is shown in decreasing difficulty to the left of the correct target-number values and in ascending difficulty to the right of the values. There are definite differences between different FOVs but not between mono and stereo vision. In fact, there was almost no difference in the total number of correctly detected targets—709 for mono vision and 712 for stereo vision. The most uniform distribution from easy to difficult occurred for the small FOV as opposed to the poor distribution for site 1 test, where 90 percent of the observers correctly identified 80 percent of the targets. This was because of the good target contrast and color discrimination during clear to partly cloudy conditions as opposed to the noisy, low-contrast scenes with muted color when it was overcast with light rain at site 2.

5.2 Observer Preference

The observer monos versus stereo preference results were collected before the observers knew how well they performed the S and TA task. The point score for mono vision was 1.92 ± 0.84 and for stereo vision 3.08 ± 0.84 . The stereo vision was preferred with a variance of over the individual populations' standard deviation, but the one standard deviation populations did overlap. For the female observer population, the results were different. The mono vision was preferred with a point score of 2.63 ± 0.92 over the stereo vision with 2.38 ± 0.92 . On the other hand, the male-observer population preferred the stereo vision with a score of 3.29 ± 0.71 to the mono vision with 1.71 ± 0.71 . In fact, the one standard deviation populations for the male observer scores did not overlap. Why then didn't the analysis of variances show any significant differences between the two techniques? As previously mentioned, the mono vision had been given a distinct advantage with the best LOS imagery and no dependence on the stereo baseline variation. Also, the analysis of variance is not designed to address the issue of multiple-target detection tasks that can better show the impact of false-target clutter. Essentially, the issue is to how to handle a scene that has a valid target and a very good false target present. The observer who is forced to pick only one may have picked both as valid targets, if given the option. Therefore, a target may be missed in this case due to limited target option. Also, if a scene has no targets and there are

two or more false targets that would have been chosen as valid targets, the results only show one false alarm and not two or more. It is necessary to view the observer results in terms of the task score based on the criteria that was given to the observers.

5.3 Observer Score

The observer score was derived from three factors as defined in the observer's general task:

1. the number of correctly identified targets,
2. the number of missed targets, and
3. the number of false target identifications.

Because the number of targets detected was so close between the mono and stereo techniques, only the number of correctly identified targets was used. The second factor of false-target detection, or false alarms (FAs), will also be addressed. A clutter rejection ratio (CR) is used that relates the number of FAs to the number of correctly ID targets by taking the ratio of the target IDs and dividing it by the total number of detections that includes the target IDs plus the FAs. This was because the targets were not of equal detection difficulty as shown in the appendix tables A-4 and A-5. Hence, an observer that has a given number of false alarms is more efficient at clutter rejection when more targets have been correctly identified compared to that number of false-target detections. The results of the overall total values and the narrow baseline, small-FOV values are shown in the appendix table A-6.

The resulting difference between the testing orders was that the scores of the group who were shown mono vision first were the worst. The low CR value translates into more FAs for this group. Both fewer correctly identified targets and lower CR for the narrow-baseline, small-FOV case are seen in the mono vision case. The results for all of the FOVs are shown in the appendix table A-4. What is of interest here is the increase in the CR of the mono vision between medium and small FOV, indicating that global clutter is beginning to cause a problem in the target-detection process.

5.4 Effects of Range and FOV

The effect of target range on detection is a variable that was not considered in the previous analysis of variance. The difference of correct target detections using stereo versus mono vision was investigated. The correct target detections using stereo minus the correct target detections using mono vision for each target location are shown in the appendix figures A-17 through A-20. Each target was shown to 18 observers. To begin looking at the individual targets that were detected, the target designation scheme needs to be given. Six target sequences were performed with four personnel in each. Therefore, the target positions were labeled as 1 through 6 and A through D. Looking at the appendix figures A-17 through A-20, there are some distinct outliers in the distributions at medium to long range that need to be investigated. These are the low points (more mono detections than stereo): target 6B at 850 m with a difference of -7 in appendix figure A-17; target 3B and 3A both at 670 m with a difference of -10 and -6, respectively, in appendix figure A-18; target 3B at 670 m with a difference of -9 in appendix figure A-19; and targets 4C, 5D, and 6B at 895 m, 850 m, and 850 m, respectively, with differences of -10, -6, and -4, respectively, in appendix figure A-20.

- Large FOV target 6B—Appendix figure A-21 shows the left and center LOS views for target 6B in the large-FOV display. This standing target has significantly more contrast in the left view than the center view on the right of appendix figure A-21. The top of this scene that has significant parallax is difficult to stereo fuse without several sessions of stereo fusion training. It appears that none of the observers successfully fused this target because there were no correct target detections; whereas, there were seven observers that keyed on the high contrast outline present in the mono (left) view of the target. The high contrast is not present in the center view (right) that was part of the stereo display pair. Without this outlier, the large FOV detections would have had only 4 targets with better mono detection than stereo and 12 targets with better stereo detection than mono and 14 more stereo detections than mono. This would have represented 16 percent better target detection with stereo.
- Medium FOV targets 3B and 3A—Appendix figure A-22 shows the left and center LOS views for these targets in the medium FOV display. In this case, the left view is much clearer than the center shown on the right of

appendix figure A-22. Also, the left view that was used as the mono display had a head feature associated with the dark blob in the line of bushes at the bottom right where target 3B is located. There is another similar target 3A with a -6 detection difference in the bottom left that was also easier to pick out in the left image than the center. Without these outliers, the medium FOV detections would have had 8+ and 8- value for the detection differences between mono and stereo vision. The stereo would have had 10 more detections, or 6 percent better target detection.

- Small FOV, narrow baseline target 3B—Appendix figure A-23 shows the left and center LOS views for this target in the small, narrow baseline FOV display. As before, target 3B has no head feature and almost no contrast in the center (on right) view of the target shown in appendix figure A-23. This target was of moderate difficulty with mono vision. Without this outlier the small, narrow baseline FOV detections would have had only five targets with better mono detection than stereo and 13 with better stereo detection than mono and 26 more stereo detections than mono. This would have represented 12 percent better target detection with stereo.
- Small FOV with wide baseline targets 4C, 6B, and 5D—Appendix figure A-24 shows the left and right views of target 4C in the small, wide baseline FOV display. This was of moderate difficulty to pick out with mono vision from the left view where the standing target silhouette can be seen in the center to top center in front of a pine tree. The right view shows very little if any silhouette for this target. Appendix figure A-25 shows the left and right views of target 6B in the small, wide baseline FOV display. The target is located in the top right of the two views but has better contrast in the left view used for the mono vision. The target was easy to detect using mono vision as 90 percent of the observers correctly identified it; whereas, only about one-half of the observers found it using stereo vision.

Two different factors might explain the difference in detection difficulty:

1. Of the eight observers who missed the target, one-half identified the large white rock in the bottom right as a target.
2. Six of the eight were right-eye dominant.

With right-eye dominance the observers get more cues from the right stereo image that had less contrast for the real target 6B and a high-contrast, false-target object. Next, appendix figure A-26 shows the left and right views of the target 5D in the small, wide baseline FOV display. The faint target is located in the center left to top left of the left view used for the mono vision. The right view used in the stereo vision pair did not have a distinct view of the target at all because it merged with a tree feature located the center and top left. There were no stereo target detections for this target. Without these outliers the wide, narrow baseline FOV detections would have had six targets with better mono detection than stereo, seven targets with better stereo detection than mono, and 11 more stereo detections than mono. This would have represented 6 percent better target detection with stereo.

As a final note, the small, wide baseline FOV target 6D outlier at 840 m with a value of +8 will be addressed. It is shown in the top right of both views in appendix figure A-27. This bush-like object was hard to detect with mono vision using the left view of appendix figure A-27. When the right and left views were used as a stereo pair display the bush-like feature stood out better and had a faint head associated with it. Thus, the volume cue stereo detection for this target was only of medium difficulty instead of hard.

The net result of this analysis is that with only minor changes to improve the display of the stereo images presented there could easily have been 10 percent more detections using stereo vision than mono vision. With an optimized display, the difference would likely be at least 20 percent more detections using stereo vision than mono vision. As illustrated by appendix figure A-19, these increases in detection will occur at longer ranges.

Another issue is the question of whether there was a difference between the ordering of the test presentation (mono vision first vs. stereo vision first and mono vision second vs. stereo vision second). Plots of the number of targets detected versus observer score are useful in seeing the difference. Appendix figures A-28 through A-31 show these plots for the four cases. Immediately apparent is that the mono vision first results have a clustering of observer results that have observers' scores between -80 and -100 instead of the other test orderings whose scores cluster in the -60 to -80 ranges. With comparable target-detection numbers for all four test orderings, which means that there had to be more false target detections using mono first than with any of the others. The CR numbers shown in appendix tables A-6 and A-7 reflects this. For the mono first results, there were twice as

many false target identifications as there were correct target identifications. The number of false target identifications is reduced for the mono vision when the stereo vision is seen first, especially for the large and medium FOVs as seen in appendix table A-7. The clutter rejection is not as good for the small FOVs, but more targets are detected.

The effects of target range can also be expressed in terms of the correct target-ID rate (i.e., the number of correct target IDs divided by the total number of targets), which are shown for the different FOVs in appendix table A-2. The difference of ID rate using stereo versus mono vision will be investigated. The mono vision and stereo vision correct target-ID rates for large, medium, small with narrow baseline, and small with wide baseline FOV images are shown in appendix figures A-32 through A-35. By looking at the individual target differences between the mono and stereo vision correct target-ID rates, it is possible to isolate several distinct outliers where the mono vision did significantly better as previously discussed. But in each case, there was a distinct difference in quality between the left image used for the mono vision test and the center or right image used as the right-eye input for the stereo image test. These outliers are

- 850-m range target in the large FOV (shown in appendix figure A-32);
- two 670-m range targets in the medium FOV (shown in appendix figure A-33);
- a 670-m range target in the small with narrow baseline FOV (shown in appendix figure A-34); and
- a 236-m, two 850-m, and an 895-m range targets in the small with wide baseline FOV (shown in appendix figure A-35).

The magnitude of the outliers can be seen better by displaying the difference (mono vision minus stereo vision) in the correct target-ID rates for both the small FOV cases (shown in appendix figure A-36). The outliers are the five values that are below -0.2 and can each be related to a display problem that gave the mono vision test a distinct advantage. Without these outliers, the stereo vision can be seen to provide several examples of improved target detection especially at the longer ranges. The net result of this analysis is that with only minor changes to improve the display of the stereo images presented. There could easily have been 10 percent more correct target IDs using stereo vision than mono vision. With an optimized display, the difference would likely be at least 20 percent more correct target IDs using stereo vision than mono vision. As illustrated by appendix figure A-36, these increases in detection will occur at longer ranges.

5.5 Clutter Rejection

The next logical step was an investigation into the characteristics of the clutter-rejection values versus the scores. Plots of observer score versus the clutter-rejection efficiency for the four observation orderings are given in appendix figures A-37 through A-40. In each case, there is a lower-limit line with positive slope that reaches the one-third value for clutter-rejection efficiency at a score of about -70. What this means is that at -70 with a one-third CR value the observer would obtain no points for target detections, because the correct target detection score (+2 for every correct identification) would be cancelled by the false target detection score (-1 for every incorrect identification). Therefore, the score is based on the missed target score (-3 for every missed target) or about 23 missed targets.

There are 45 or 46 targets shown in the different tests administered to the four orderings of the observer tests; thus, the -70 score with one-third efficiency represents about the 50 percent target detection position for the overall test. There is some upward migration of the observer-score distribution along the lower-bound line for mono vision first near the middle. The upward migration of the score distribution away from the lower-bound line for the mono second is definitely concentrated in the better score region to the right of the 50 percent detection position with the overall distribution moving to the right. The upward migration of the score distribution away from the lower-bound line for the stereo first is also concentrated in the better score region to the right of the 50 percent detection position with the overall distribution showing marked movement to the right.

Finally, the upward migration of the score distribution away from the lower-bound line for the stereo second occurs everywhere except in the lower-score region with a thoroughly marked movement of the distribution to the right. The comparison of these four plots shows that there is definitely an overall improvement shown in target-clutter rejection efficiency in the better score region by every test ordering except mono first.

The next step in the analysis of the clutter rejection was to define a function that has better characteristics over the observer score distribution than just the ratio of correct-target detections divided by the total number of target detections. The problem is that the targets do not all have the same difficulty in detection associated with them as seen in appendix tables A-4 and A-5. If the average number of target detections is 5 with a CR of one-third, an observer that detects 8 targets with 16 false alarms has done a much better job of clutter rejection than an observer who has only

detected 2 targets with 4 false targets. However, both of their CR values would have been one-third. An initial detection and clutter-rejection measure (D/CRM) was defined that incorporates all of the above issues. The basic idea is to perform a vector addition of the score, which is highly correlated to the correct target detections, and clutter rejection efficiency values normalized about the mean and standard deviation of the mono-first distribution. Hence, if the score (-63) were higher (better) than the mean mono-first distribution by one mono first standard deviation (± 19) of the mono first score distribution (-82 ± 19), then the score portion of the D/CRM would be 1. If the clutter rejection efficiency (0.41) were higher (better) than the mean mono-first distribution by one mono first standard deviation (± 0.08) of the mono first clutter rejection efficiency distribution (0.33 ± 0.08), then the clutter rejection efficiency portion of the D/CRM would also be 1. These vector values would combine to give an overall detection and clutter rejection measure value of 1, which is normalized by the $\sqrt{2}$. If the score were -101, then the score portion of the D/CRM would be -1; and the D/CRM would be 0. For the case where the score and clutter-rejection portions have opposite signs, the square root of the magnitude of the difference of the two vector components is taken and the result divided by the $\sqrt{2}$. The D/CRM thus defined had a problem. The value of the clutter-rejection efficiency was not properly bound. With possible values ranging from 0 to 1, the clutter-rejection portion of the D/CRM could take on values of -4 to +8.

To correct this lopsided bounding and take into consideration the issue of how many targets were detected when obtaining the clutter-rejection efficiency value, the average number of detected targets for the mono first tests was used. The clutter-rejection value portion of the new D/CRM was weighted by the square of the ratio of the number of correct targets identified, divided by the average number of targets detected in the mono first test. There is a proviso that if the number were greater than one the weighting enhancement would not be applied when the clutter rejection efficiency was already larger than four standard deviations above the mean clutter-rejection efficiency (i.e., 0.67). When this was done, a well-behaved function was obtained. The overall mono first distribution of D/CRM values had two-thirds within one standard deviation of the average value, and one-sixth both one-to-two standard deviations above and below the average value. The D/CRM was then plotted against the observer score to obtain a straight-line plot for the mono first case and straight lines with minor variations for the other presentation orderings as shown in appendix figures A-41 through A-44.

Now, the deviations as a function of score can be better seen between the mono first and the other presentation orderings. The portion of the mono first observer distribution that received better scores did worse in rejecting false targets than any of the other presentation orderings for all of the FOVs combined. The question becomes, then, how did stereo vision training impact stereo vision performance? From the comments made by the observers and noting the reactions to rating the ease of fusing the scenes, the observers' ability to use stereo vision improved significantly during the course of the test that lasted a little over an hour. The stereo training portion given prior to the test lasted only about 15 min. The large/medium FOV portion of the test was given first and then the small FOV portion.

If the observers were improving their use of stereo vision during the testing, there may be improvement in the use of stereo vision that shows up between the large and medium FOV portion of the test and the small FOV portion that is not related to the FOV size difference. Alternately, the observers may have performed better on the large and medium FOV portion of the test had they had more stereo vision training. To see these effects, the observer score versus the large FOV D/CRM are shown in appendix figures A-45 through A-48. Here, there is more scatter because of the smaller sample size, but the plots do not show the marked upward migration of the distribution seen in the overall, FOV test results for the mono second, stereo first, and stereo second that are present in appendix figures A-42 through A-44. Rather than show all of the FOV plots separately, the ratios of the D/CRM for the other presentation orderings to that of the mono first are shown for the four different FOVs in appendix figures A-49 through A-52. Here, for the large FOV (shown in appendix figure A-52) some detection improvement is evident since the data forms a line whose slope is larger than 1 with a negative x-axis intercept. Also, only the observers with the poorest clutter rejection (the left end of the distribution) had values that fell below a line of slope 1.0, passing through the origin that would represent no difference in the large FOV results as a function of presentation order. For the medium FOV (shown in appendix figure A-50), there is a more pronounced improvement especially for the right side of the distribution, and again, only the left end of the distribution showed poorer results. The small, narrow baseline FOV (shown in appendix figure A-51) gave the best results; even the left end of the distribution where the clutter rejection results were the worst did better. For the small, wide baseline FOV (shown in appendix figure A-52), the observers did not perform better using stereo on the left end where the scores were poorest. However, for those observers who could use stereo, the results were quite good as seen on the right end of the distribution.

Finally, because the small FOV, narrow and wide baseline was obtained simultaneously in the second portion of the stereo test, the combined results are shown in appendix figure A-53. Here there is much less variation in the results because of the larger sample size. The transition from the poorer results for the left end of the distribution to better results on the right end of the distribution can be clearly seen for the two stereo cases that track each other very well. The mono second results can be seen to be better for the right end of the distribution but not as good as the stereo vision results. These results indicate that about a factor of 2 reduction in the false alarms may be possible to achieve if sufficient training in the use of stereo vision and optimized display of the scenes are performed.

The last issue to be addressed is the false target detections, or false alarms. As can be seen from the CR values in appendix table A-7, the ratio of false alarms compared to correct target detections decreased from about 3 to 1 with the wide FOV for the mono vision first case to about 1.5 to 1 for the medium FOV. As mentioned before, it appears that the narrow vision FOV global clutter may have become a problem for the mono vision first case since the ratio of false alarms to correct detections dropped to a little over 2 to 1. Therefore, the narrow FOV cases will be considered. As mentioned above, the average number of targets detected were fairly close. Using mono vision, there were 12.08 ± 2.23 correct target detections out of 23 possible targets; using stereo vision there were 12.36 ± 2.05 . The average numbers of false alarms were considerably different between mono and stereo vision. Using mono vision, there were 24.64 ± 11.44 false alarms for the small FOV cases; whereas, for stereo vision there were only 18.72 ± 11.06 . This represents only an average of 25 percent decrease in false alarms, but the distribution is quite different for those observers in the upper half of the distribution compared to the lower half. Appendix figures A-54 and A-55 compare the numbers of false alarms between all 36 observers between mono and stereo vision for the combined small FOV cases. In appendix figure A-54, one-half of the distribution that performed better (fewer false alarms) represented mono vision scores of 25 or less. In this portion of the curve, the slope ranges from about one-half to two-thirds or from 33- to 50-percent decreases in false alarms. In the other one-half of the distribution, the slope becomes > 1 and shows far less difference in false alarms between those observers who were not able to use stereo vision effectively). For stereo vision compared to mono vision, there is a significant overall drop in the number of the false target detections or FAs for the small

FOV scenes shown in appendix figure A-55. These results indicate that the number of FAs may be decreased by a factor of 2, if sufficient training using stereo vision is given to the observers prior to testing.

Conclusions

An S and TA test was conducted that provided single and wide baseline stereo imagery for observer testing. The database contains the same scene with and without camouflaged human targets present. The analysis of imagery from the second of two sites has resulted in several interesting findings. Analysis of variance did not show significant differences between mono vision and stereo vision in general; however, there were differences in the observer responses. First, there was a significant difference in the false-target detections between mono and stereo vision for the narrow FOV cases. Second, analysis of the effect of target range showed that for the small, narrow-baseline FOV case there was a better performance with longer ranges. Also, there were several targets that could be identified as distribution outliers and rationale for the poorer performance of the stereo vision related to biased displays that favored the mono vision. There was only a little difference in the total number of correctly detected targets. Nonetheless, there is reason to believe that an approximate 20-percent increase in correctly identified targets, using stereo vision, may be possible to obtain if proper training in the use of stereo vision is given prior to testing and optimized displays are used. Third, it appears that as the FOV was decreased from the medium to small, the mono vision experienced an increase in false alarms, possibly from the effects of global clutter. About one-half of the observers showed a substantial decrease in false alarms indicating again, that, with proper training in the use of stereo vision and optimized displays, the number of false alarms may be decreased by a factor of 2 using stereo vision. Finally, data were obtained that can be used to optimize the display for observer performance using stereo vision.

Further testing is required to obtain results that show analysis of variance significance for stereo vision over mono vision. There were too many nuisance factors in the present observer experiment that could now be eliminated or greatly reduced by performing further observer tests based on the results presented here. The testing should concentrate on the small, narrow baseline FOVs with targets at ranges of 500 m or more with either one or no targets present. The displays from the two LOS should be shown such that any differences in mono vision performance can be identified and compared to stereo displays that normalize out the effects of observer eye dominance. The observers should be divided into two groups and only shown the mono or the stereo test. Finally, the observers must be adequately trained

using stereo vision before the S and TA test is performed. These tests could be performed at the U.S. Military Academy where there is faculty interest in participating in the experiments and a reasonable observer base that can be utilized.

References

1. CuQlock-Knopp, V.G., et al., *Human Off-Road Mobility, Preference, and Target-Detection Performance With Monocular, Binocular, and Binocular Night Vision Goggles* (U), U.S. Army Research Laboratory, Technical Report ARL-TR-1170, 2800 Powder Mill Road, Adelphi, MD, 20783-1190 (1996). UNCLASSIFIED
2. Merritt J.O., R.E. Cole and C. Ikehara, *A Rapid Sequential Positioning Task for Evaluating Motion Parallax and Stereoscopic 3D Cues In Teleoperator Displays* (U), 1991 IEEE Conference on Systems, Man, and Cybernetics, University of VA, Charlottesville, VA, pp. 1041-1046 (1991). UNCLASSIFIED
3. Papathomas, T.V., et al., *Early Vision and Beyond* (U), The MIT Press, Cambridge, MA (1994). UNCLASSIFIED
4. Marr D. and T. Poggio, "A Computational Theory of Human Stereo Vision (U)," In *Proceedings R. Soc. Lond. B.*, **204**, pp. 301-328 (1979). UNCLASSIFIED
5. Woods A., T. Docherty and R. Koch, "Image Distortions in Stereoscopic Video Systems (U)," In *Proceedings SPIE*, **1915** (1993). UNCLASSIFIED
6. Jahne B., *Practical Handbook on Image Processing for Scientific Applications* (U), CRC Press, Boca Raton, FL (1997). UNCLASSIFIED
7. Watkins W.R., "Multispectral Image Processing: The Nature Factor (U)" In *Proceedings SPIE*, **3545**, pp. 4-7 (1998). UNCLASSIFIED
8. Bijl P., F.L. Kooi and J.M. Valeton, *Visual Search Performance for Realistic Imagery from the DISSTAF Field Trials* (U), (Report TM-97-A055), TNO Human Factors Research Institute, Soesterberg, The Netherlands (1997). UNCLASSIFIED
9. Watkins W.R., J.B. Jordan and M.M. Trivedi, "Novel Applications of Hyper Stereo Vision (U)," In *Proceedings SPIE*, **3310**, pp. 72-88 (1997). UNCLASSIFIED
10. Ratches J.A., "Night Vision Modeling: Historical Perspective (U)," In *Proceedings SPIE*, **3701**, pp. 2-12 (1999). UNCLASSIFIED

11. Watkins W.R and L. Alaways, "Depth Perception Applied to Search and Target Acquisition (NATO U), NATO RTO Meeting In *Proceedings on Search and Target Acquisition Workshop* (RTO-MP-45/AC/323(SCI)TP/19), BP 25, 7 Rue Ancelle, F-92201 Neuilly-Sur-Seine Cedex, France (2000). NATO UNCLASSIFIED
12. The Institute for Perception TNO, *TNO Test for Stereoscopic Vision* (U), 8th edition, Lameris Instrumenten b.v., Biltstraat 449, 3572 aw Utrecht, The Netherlands (1972). UNCLASSIFIED
13. Heath G., W.R. Watkins and M.D. Phillips, "A Comparison of Observer Task Performance: Three Dimensional Versus Two Dimensional Displays (U)," *Proceeding of the Eighth Annual USARL/USMA Tech. Sym.*, Mathematical Sciences Center of Excellence, United States Military Academy, West Point, NY, 199-208 (2000). UNCLASSIFIED

Acronyms

3D	three dimensional
ANOVA	Analysis of the Variance
ARL	U.S. Army Research Laboratory
DISSTAF	Distributed Interactive Systems Search & Target Acquisition Fidelity
CR	clutter rejection
D/CRM	detection and clutter-rejection measure
FA	false alarm
FOV	field of view
ID	identification
LOS	line of sight
SEDD	Sensors & Electron Devices Directorate
S	search
TA	target acquisition
TNO	The Netherlands Organization for Applied Scientific Research
USMA	U.S. Military Academy

**Appendix. Search and Target Acquisition: Single Line of Sight
Versus Wide Baseline Stereo Figures and Tables**

Figure A-1. The four TNO personnel with forest camouflage used as targets.



Figure A-2. The three stereo camera setup with 10-m baseline separation used at site 2.

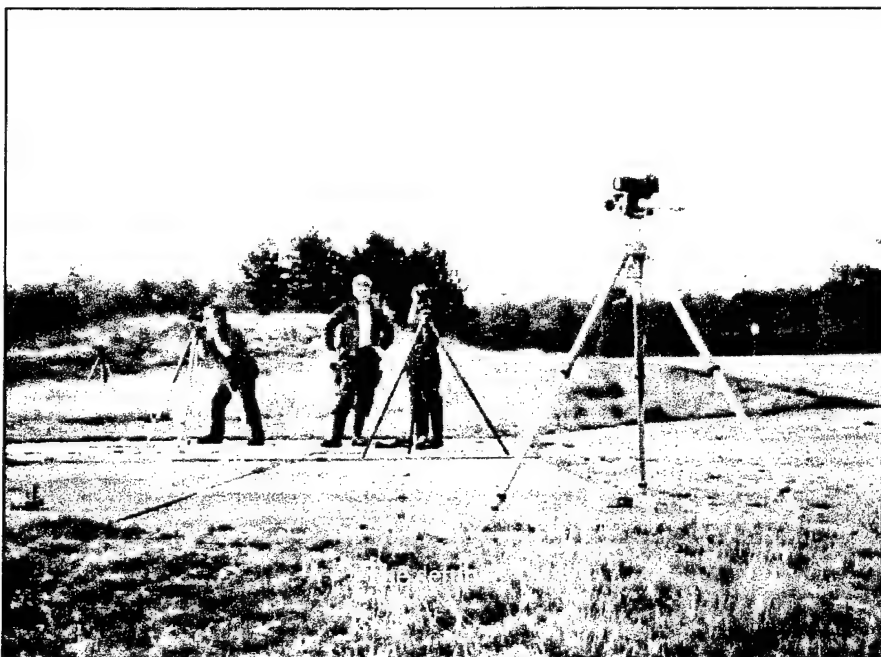


Figure A-3. Whole scene from site 1 with no targets.

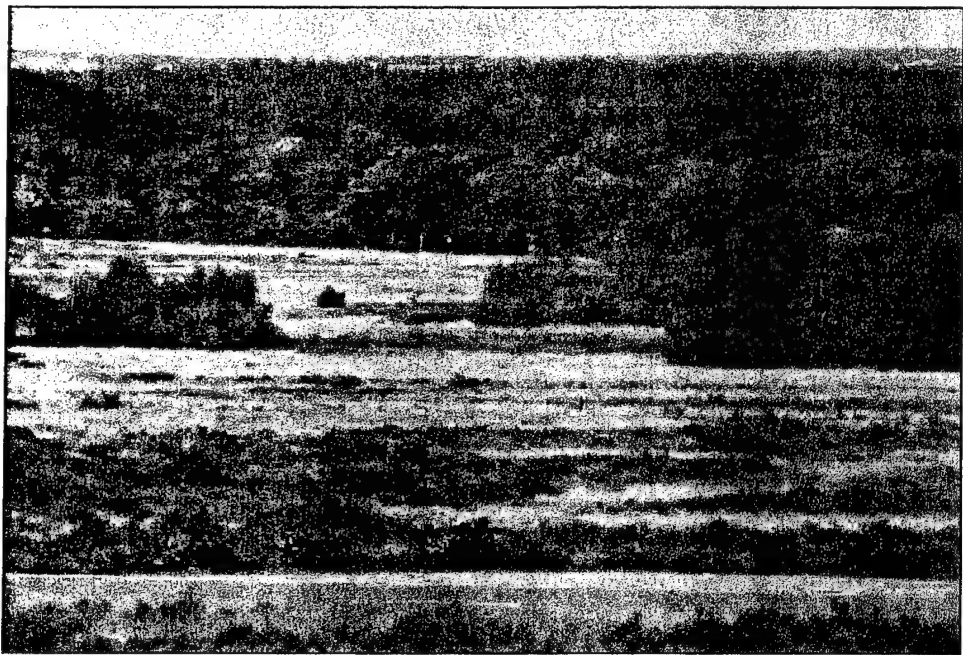


Figure A-4. Site 1 with target positions designated with large white cards.



Figure A-5. Whole scene from site 2 with no targets.



Figure A-6. Site 2 with target positions designated with large white cards.



Table A-1. The 7 x 4 array of target sectors

Target Sectors	A1	A2	A3	A4	A5	A6	A7
B1	B2	B3	B4	B5	B6	B7	
C1	C2	C3	C4	C5	C6	C7	
D1	D2	D3	D4	D5	D6	D7	

NOTE:

Used for site 1 with nominal ranges to the ground level within the sectors of 130 m to 180 m in row D, 180 m to 340 m in row C, 340 m to 520 m in row B, and 520 m to 675 m in row A.

Table A-2. FOVs used for the site 2 test

FOV size	Number of grid blocks	Sectors used for targets
Small (50% smaller) 192 X 120 pixels	8 wide by 5 high	20 with 23 targets Group A: 10 with 12 targets Group B: 10 with 11 targets
Medium (standard size) 384 X 240 pixels	16 wide by 10 high	12 with 23 targets Group 1: 6 with 12 targets Group 2: 6 with 11 targets
Large (50% larger) 576 X 360 pixels	24 wide by 15 high	10 with 22 targets Group 1: 5 with 10 targets Group 2: 5 with 12 targets

NOTE:

The small FOV had Groups A or B displayed with the 10-m baseline and the other group with the 20-m baseline. The medium and large FOVs were combined for one portion of the test with either Groups No. 1 or 2 that contained either 22 or 23 different targets.

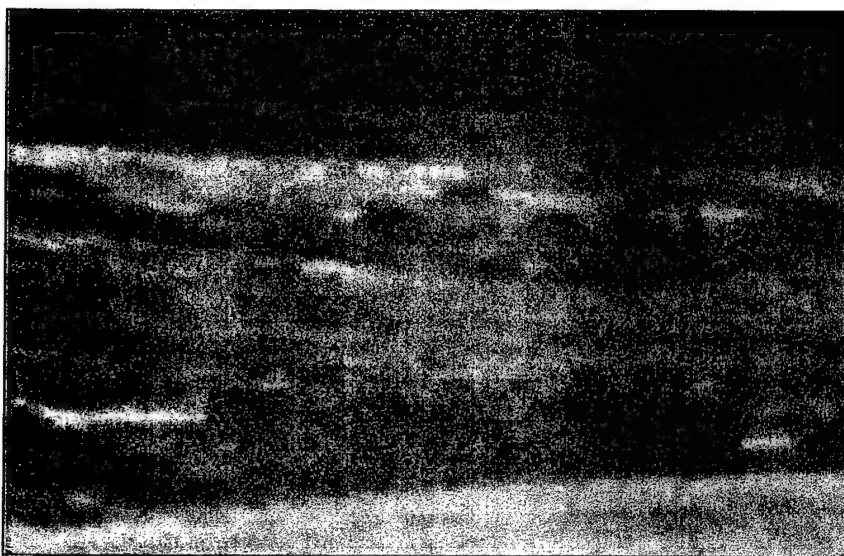
Figure A-7. Large FOV scene with three targets present.



NOTE:

The most conspicuous target is crouching just to the left of the concrete bunker in the bottom of the scene. The other two targets are in the center and upper right.

Figure A-8. Medium FOV scene with five targets present.



NOTE:

There is only one obvious standing target in the center right.

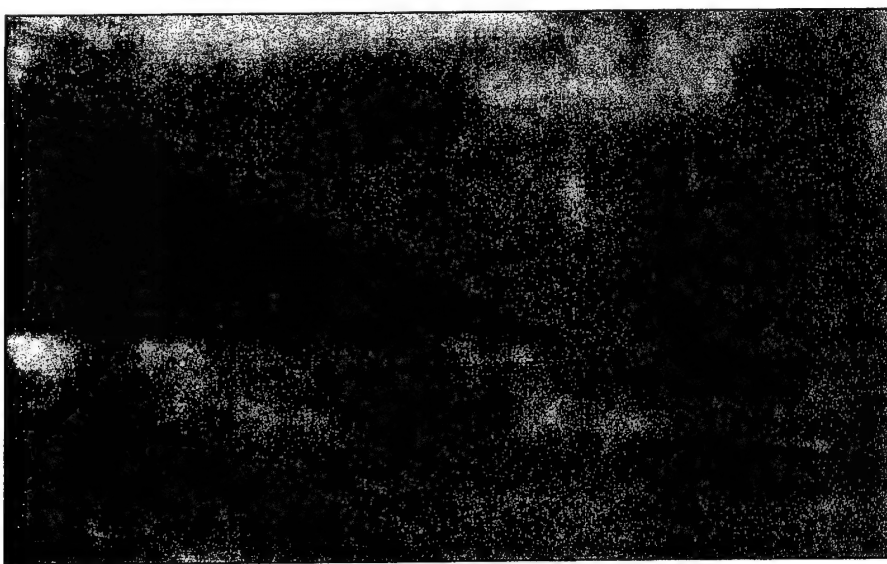
Figure A-9. Medium-FOV scene with two squatting targets present.



NOTE:

There is one easy target in the lower left portion of the scene and a very difficult target just on the far side of the road between top left and top center.

Figure A-10. Small FOV scene with one large squatting target present.



NOTE:

Small FOV scene with a large target squatting in the center right and a very similar false target in the lower left.

Table A-3. Distribution of correct target detections by the observers for a particular target for site 1

Problems with first site	
Number of targets	Number of correct detections out of 30
19	27 - 30
1	16 - 26
3	12 - 15
1	0 - 3

NOTE:

The targets were too easy to detect and the stereo display did not work at ranges of less than 300 m.

Figure A-11. One of the moderately difficult targets in the squatting position at 550 m in the lower center of the scene under clear sky conditions from site 1.



Figure A-12. Another moderately difficult target from site 1 is shown squatting in the lower center of the scene at 375 m.



Figure A-13. An easy standing target is shown in the center left at 450 m and a second moderately difficult target to the left of the big bush in the top left at 475 m.



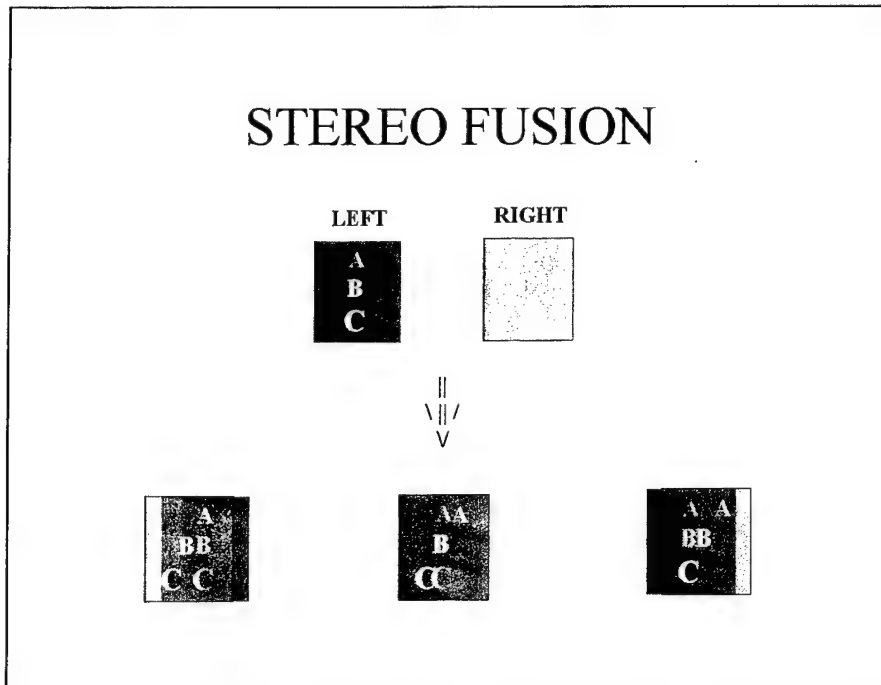
Figure A-14. An easy standing target is shown in the center left at 450 m and a second moderately difficult target to the left of the big bush in the top left at 475 m.



Figure A-15. This is a panoramic view of the entire first site with no targets present with the near road at 100 m and the far road at 650 m.



Figure A-16.
Example of how
scenes must be
merged differently
top to bottom when
observer views the
objects *A*, *B*, and *C* in
stereo.



NOTE:

The observers have different parallax between the left and right images.

Table A-4. Difficulty in correctly detecting targets in site 2 scenes using mono vision

Detection difficulty mono LOS				
Efficiency	LM	MM	SNM	SWM
0.86 – 1.00	1	3	5	6
0.70 – 0.85	2	4	E 4 M	E 5 M
0.53 – 0.69	0	E 2 M	3	1
0.36 – 0.52	3	2	3	1
0.20 – 0.35	E 3 M	2	M 2 H	M 3
0.00 – 0.19	M 13 H	M 10 H	6	7 H

NOTES:

1. Abbreviations:
 - E - Easy
 - M - Medium
 - H - Hard
2. Acronyms:
 - LM - Large Mono
 - MM - Medium Mono
 - SNM - Small Narrow Baseline Mono
 - SWM - Small Wide Baseline Mono
3. The results are as a function of FOV and correct target ID efficiency (fraction of the observers making correct target ID). The entries are the correct target IDs. Here there is no difference between the small, narrow mono SNM and small, wide mono SWM scenes displayed.

Table A-5. Difficulty in correctly detecting the targets in site 2 scenes using stereo vision

Detection difficulty stereo LOS				
Efficiency	LS	MS	SNS	SWS
0.86 - 1.00	1	3	E8	6
0.70 - 0.85	2	E5	3M	E 5 M
0.53 - 0.69	2	0	1	3
0.36 - 0.52	E2	5M	2	1
0.20 - 0.35	2 M	2	M 4 H	M 4 H
0.00 - 0.19	M 13 H	M 8 H	5	6

NOTES:

1. Abbreviations:

E - Easy

M - Medium

H - Hard

2. Acronyms:

LS - Large Stereo

MS - Medium Stereo

SNS - Small Narrow Baseline Stereo

SWS - Small Wide Baseline Stereo

3. The results are as a function of FOV and correct target-ID efficiency.

Table A-6. Observer task results showing the scoring results for the different testing order first (f) and second (s) for the combined FOV and narrow baseline, small FOV

S and TA results			
Mono (f)	Stereo (f)	Mono (s)	Stereo (s)
All FOVs			
45 or 46 targets			
T = 19.2	T = 20.8	T = 20.2	T = 19.2
CR = .33	CR = .41	CR = .39	CR = .45
S = -82	S = -68	S = -73	S = -68
Small/narrow FOV			
11.5 targets			
T = 5.6	T = 6.6	T = 6.5	T = 6.6
CR = .34	CR = .44	CR = .37	CR = .48
S = -20	S = -12	S = -14	S = -10

NOTE:

T - Targets

CR - Clutter Rejection

S - Score

Table A-7. Observer task results show scoring results for the different testing order, first (f) and second (s) for the combined FOV and narrow baseline, small FOV

S and TA results			
Mono (f)	Stereo (f)	Mono (s)	Stereo (s)
Large FOV			
T = 2.9	T = 3.2	T = 2.4	T = 2.5
CR = .28	CR = .34	CR = .34	CR = 1
S = -27	S = -25	S = -27	S = -26
Medium FOV			
T = 4.9	T = 5.0	T = 5.0	T = 4.6
CR = .38	CR = .44	CR = .47	CR = .49
S = -19	S = -16	S = -16	S = -17
Small/narrow FOV			
T = 5.6	T = 6.6	T = 6.5	T = 6.6
CR = .34	CR = .44	CR = .37	CR = .48
S = -20	S = -12	S = -14	S = -10
Small/wide FOV			
T = 5.8	T = 6.0	T = 6.3	T = 5.5
CR = .36	CR = .42	CR = .37	CR = .48
S = -17	S = -15	S = -16	S = -15

NOTE:

T - Targets
 CR - Clutter Rejection
 S - Score

Figure A-17. Plot of correct target detections (stereo/mono) as a function of target range for the large FOV.

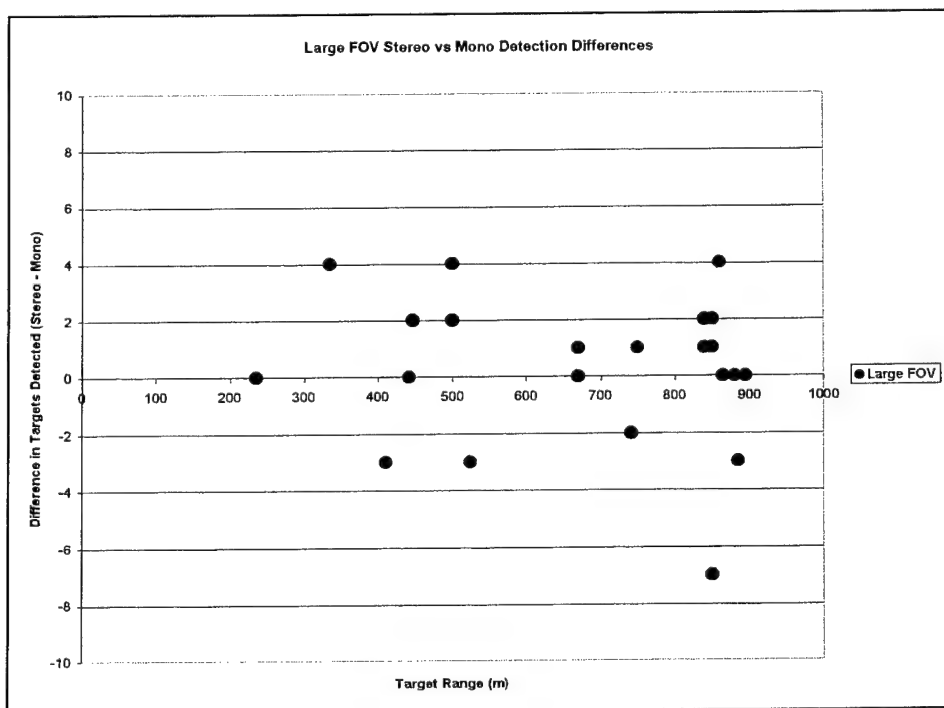


Figure A-18. Plot of correct target detections stereo/mono as a function of target range for medium FOV.

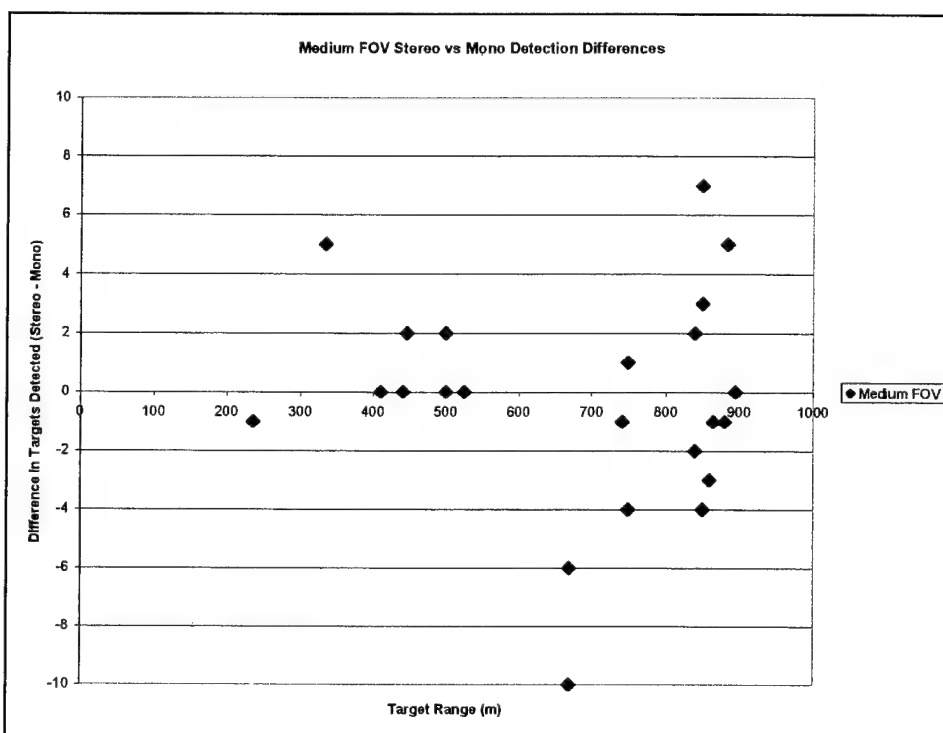


Figure A-19. Plot of correct target detections stereo/mono as a function of target range for the narrow baseline, small FOV.

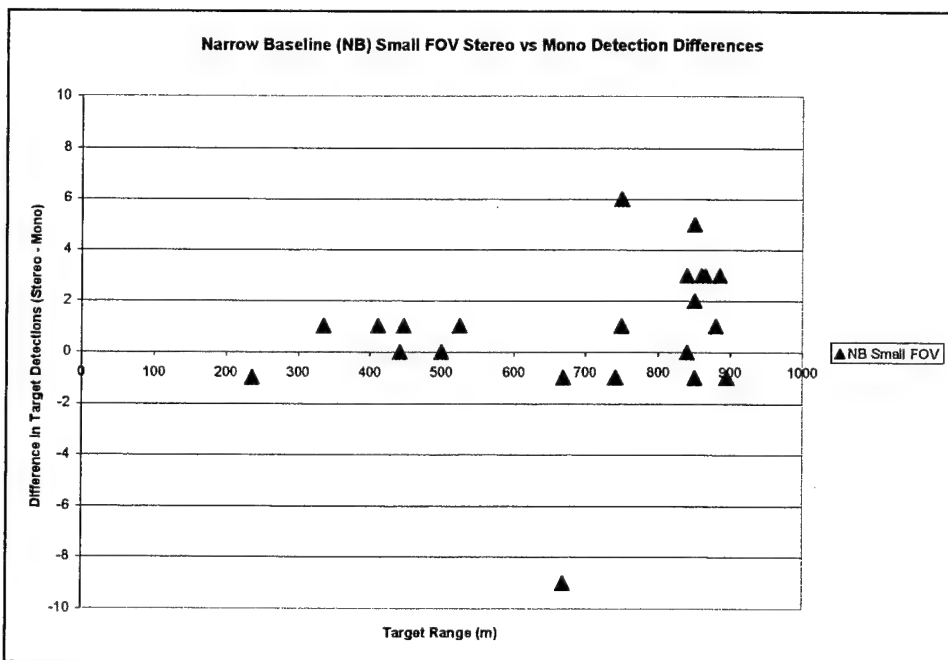


Figure A-20. Plot of correct target detections (stereo/mono) as a function of target range for the wide baseline, small FOV.

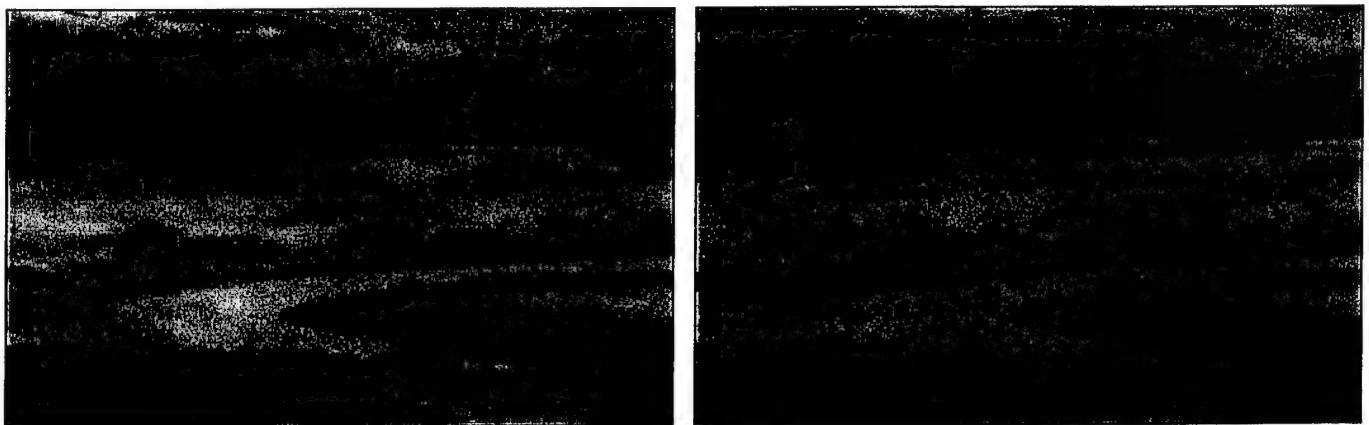
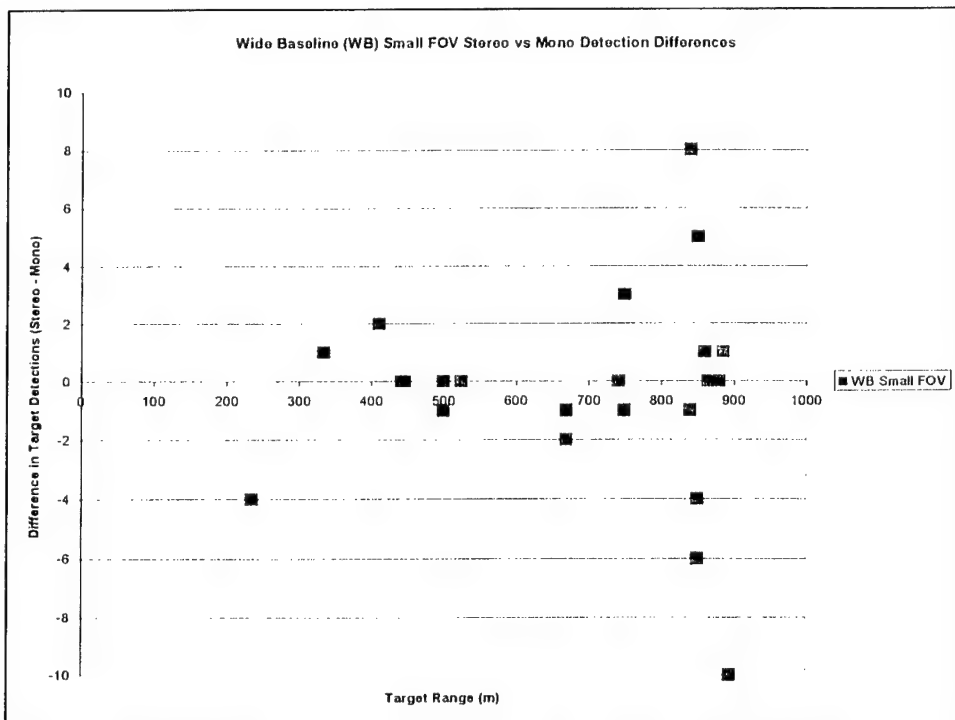


Figure A-21. Left (on left) and center (on right) large FOV of the scene containing target 6B (top right to top center of left view).

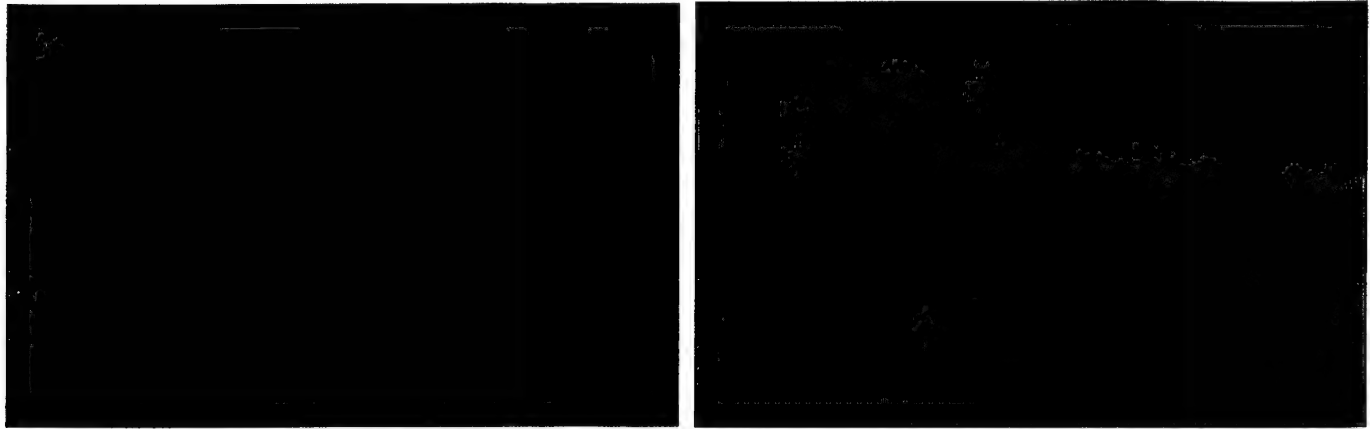


Figure A-22. Left (on left) and center (on right) medium FOV of the scene containing target 3B (bottom left of both views).

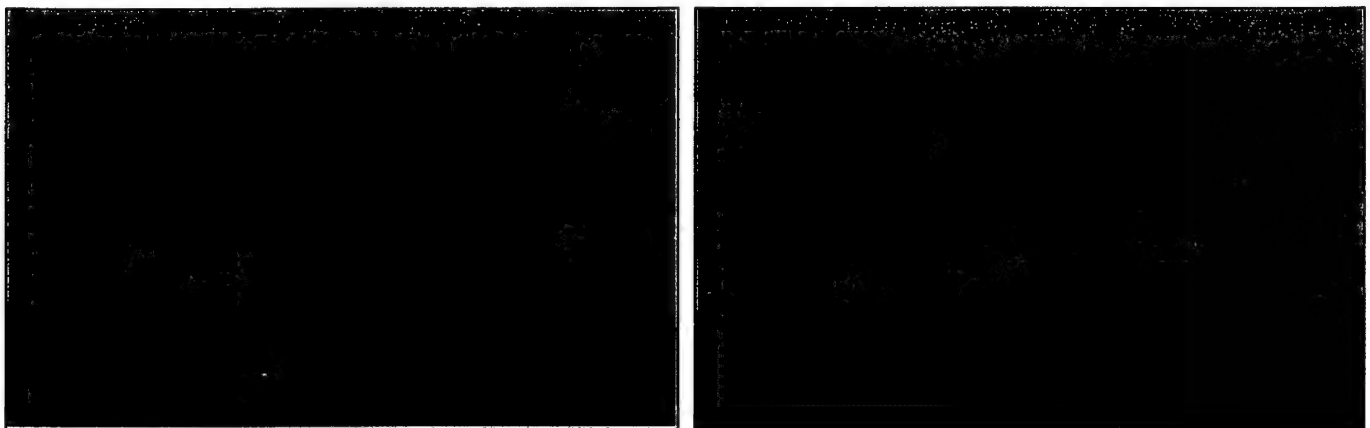


Figure A-23. Left (on left) and center (on right) small, narrow baseline FOV of the scene containing target 3B (top left of left view).

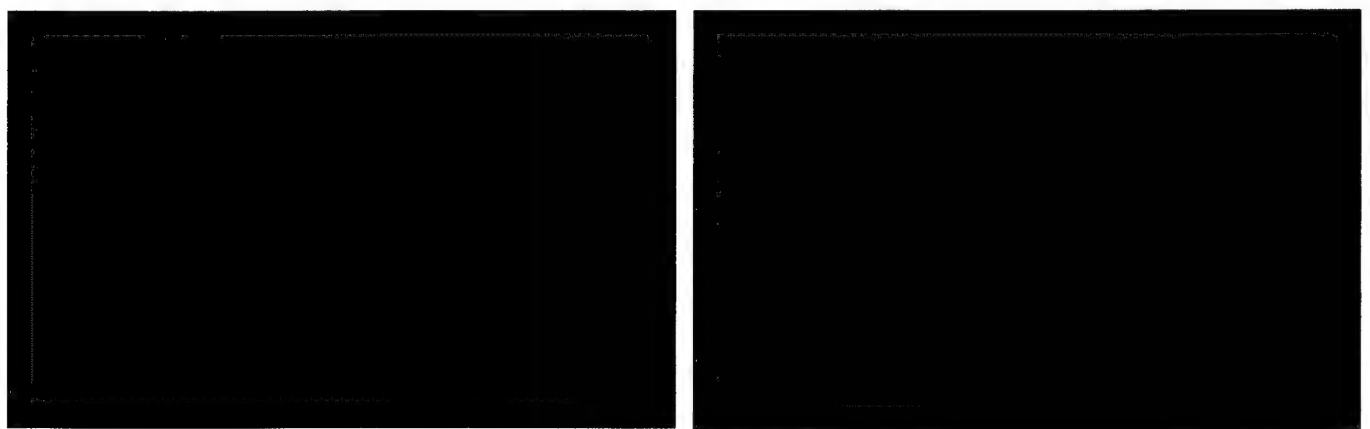


Figure A-24. Left (on left) and right (on right) small, wide baseline FOV of the scene containing target 4C (center to top center in standing in front of a bush).

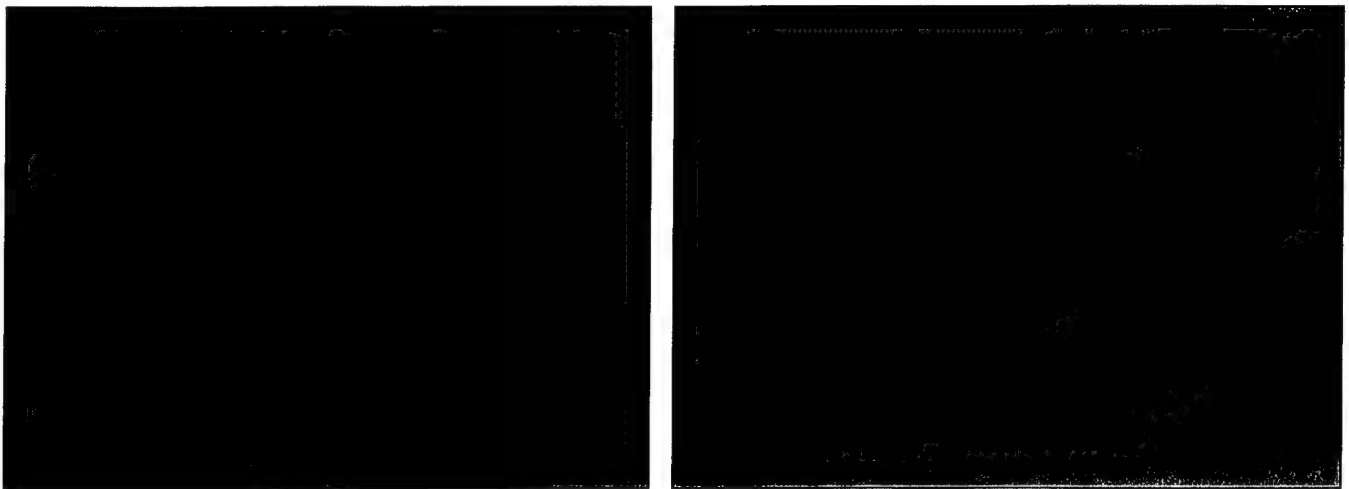


Figure A-25. Left (on left) and right (on right) small, wide baseline FOV of the scene containing target 6B (top left in both).

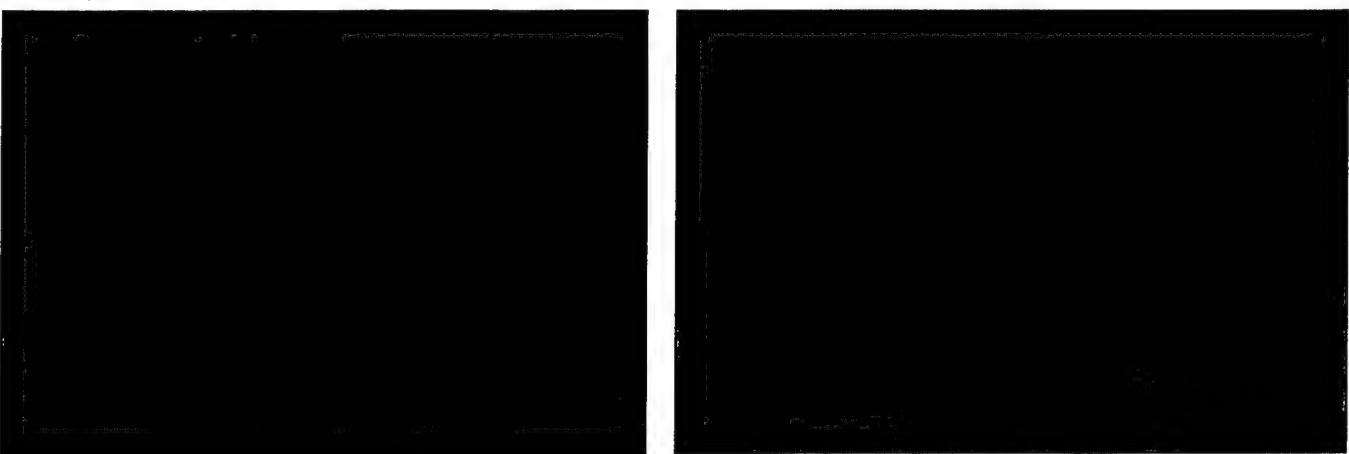


Figure A-26. Left (on left) and right (on right) small, wide baseline FOV of the scene containing target 5D (top left of the left view).

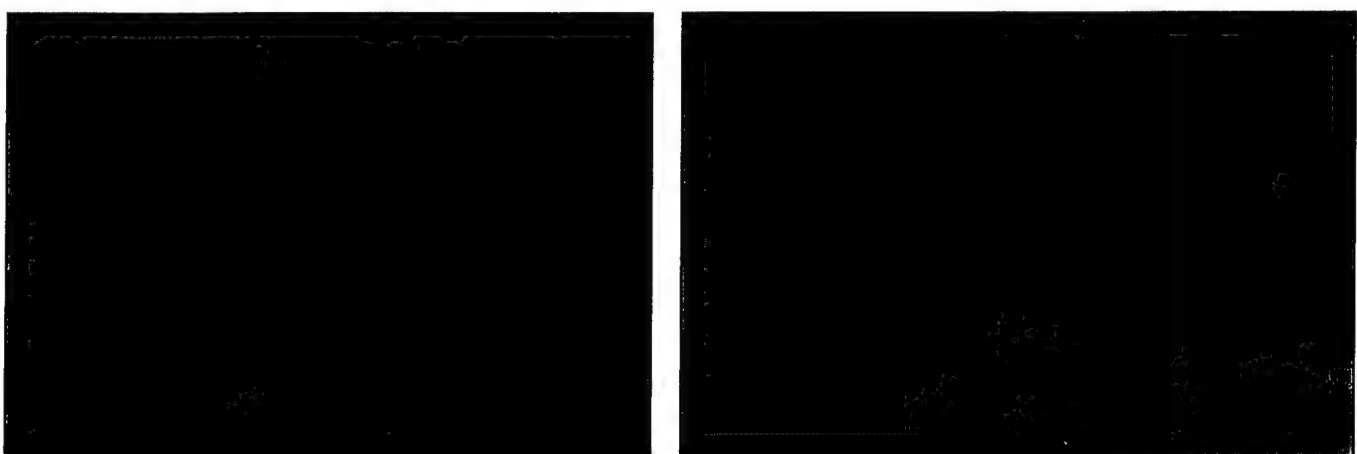


Figure A-27. Left (on left) and right (on right) small, wide baseline FOV of the scene containing target 6D (top right of both views).

Figure A-28. Plot of observer score versus detected targets for the mono vision performed first.

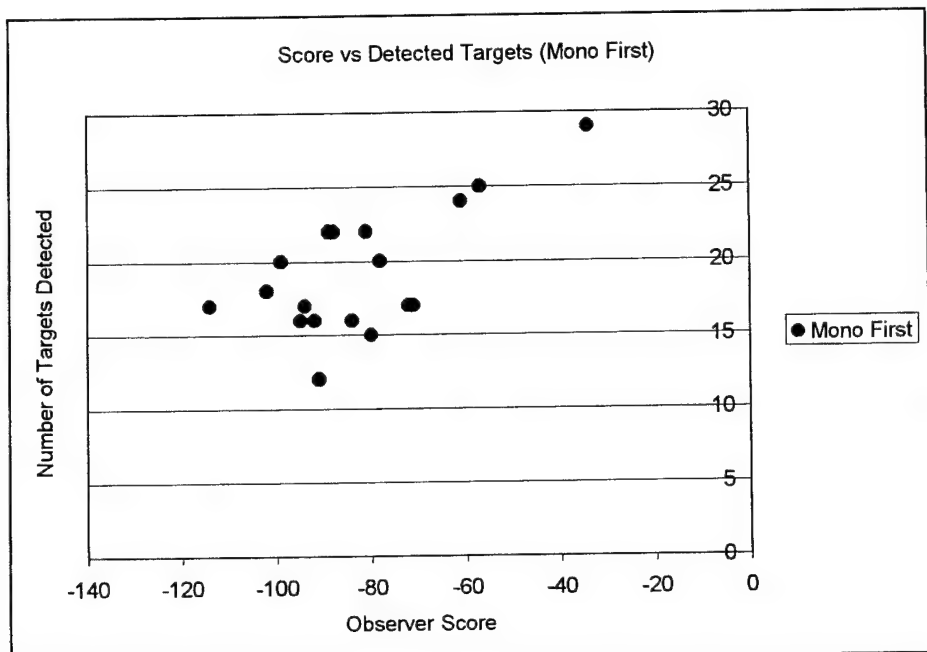


Figure A-29. Plot of observer score versus detected targets for the mono vision performed second.

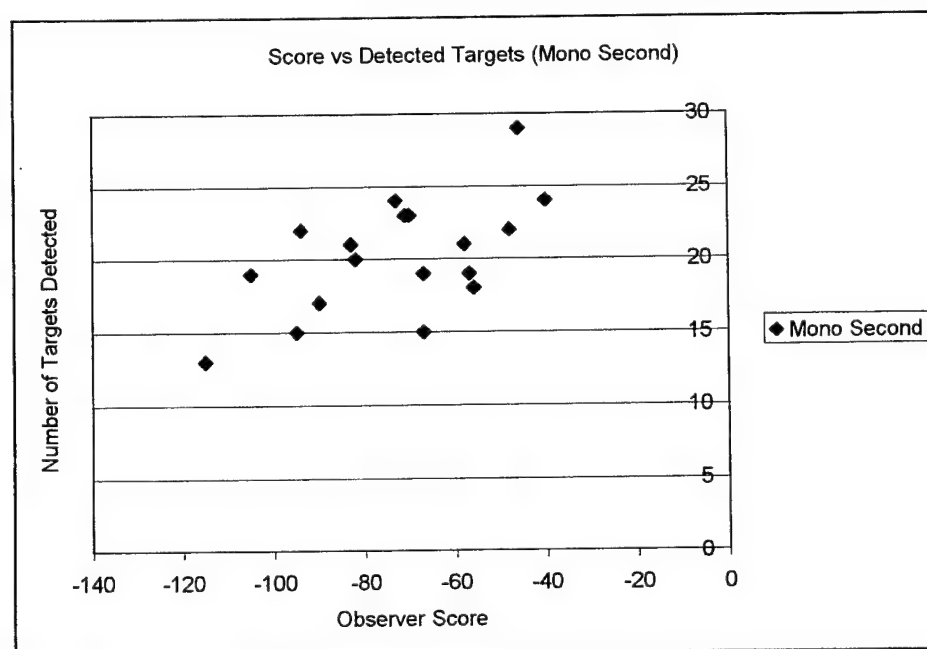


Figure A-30. Plot of observer score versus detected targets for the stereo vision performed first.

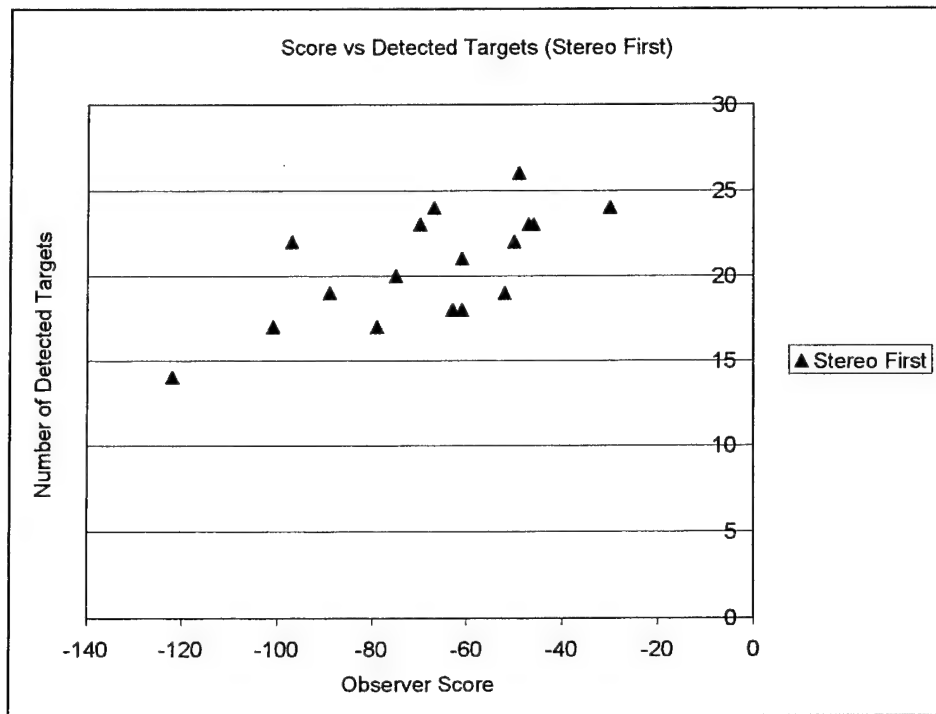


Figure A-31. Plot of observer score versus detected targets for the stereo vision performed second.

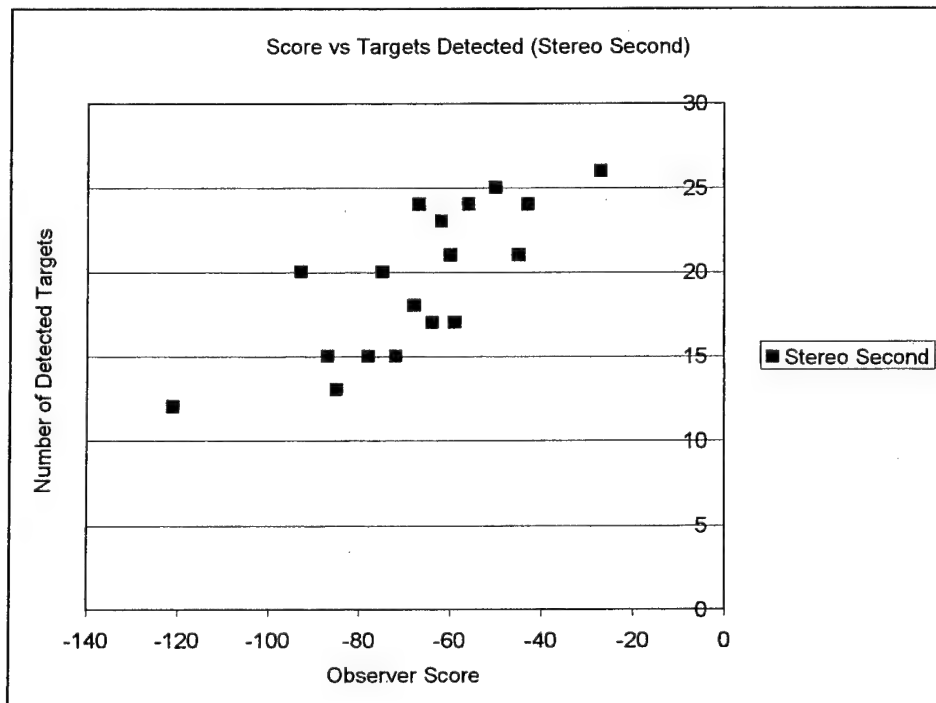


Figure A-32.
Comparison of mono versus stereo vision for correct target ID rate for the large FOV scenes.

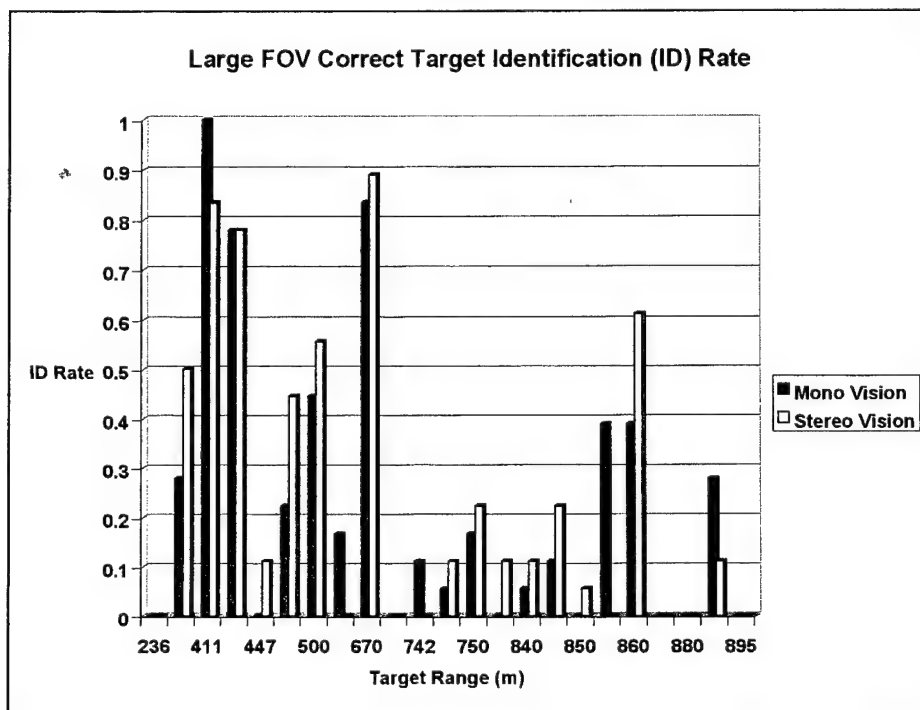


Figure A-33.
Comparison of mono versus stereo vision for correct target ID rate for the medium FOV scenes.

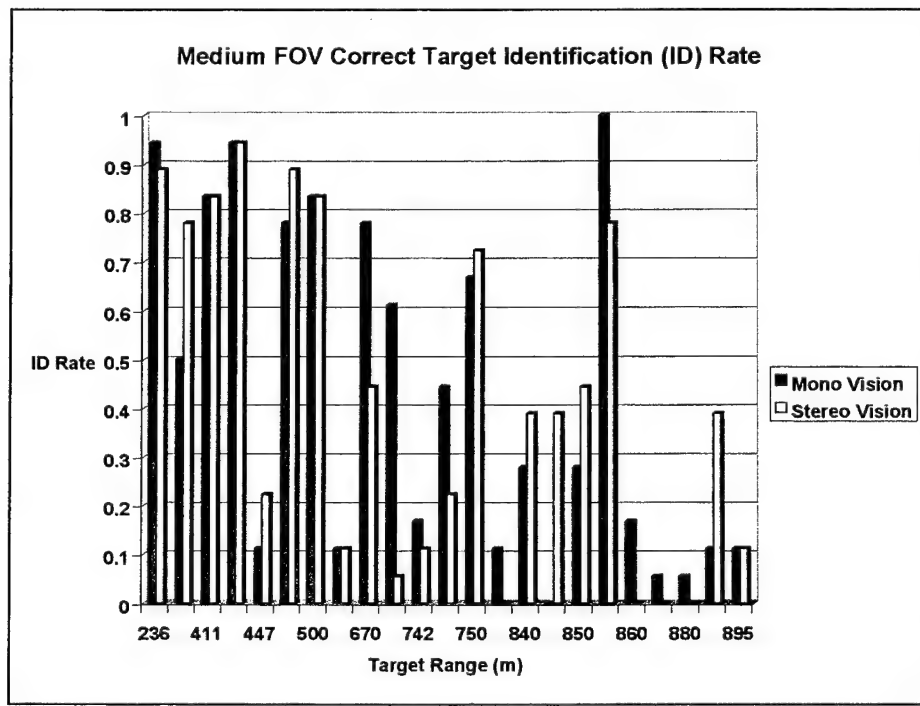


Figure A-34.
Comparison of mono versus stereo vision for correct target ID rate for the small FOV scenes with narrow stereo baseline.

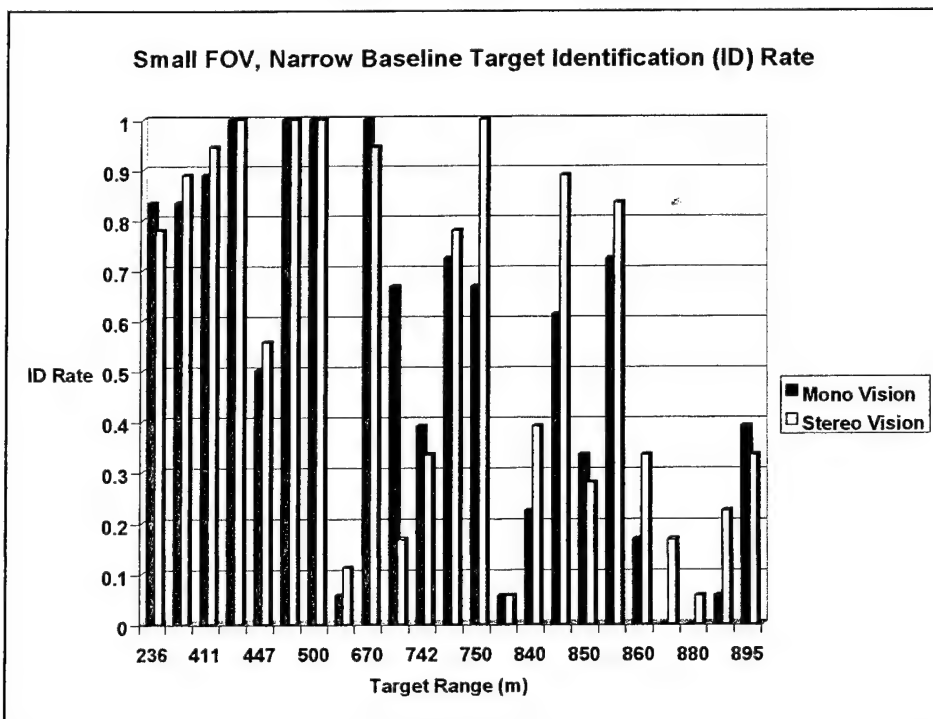


Figure A-35.
Comparison of mono versus stereo vision for correct target ID rate for the small FOV scenes with wide stereo baseline.

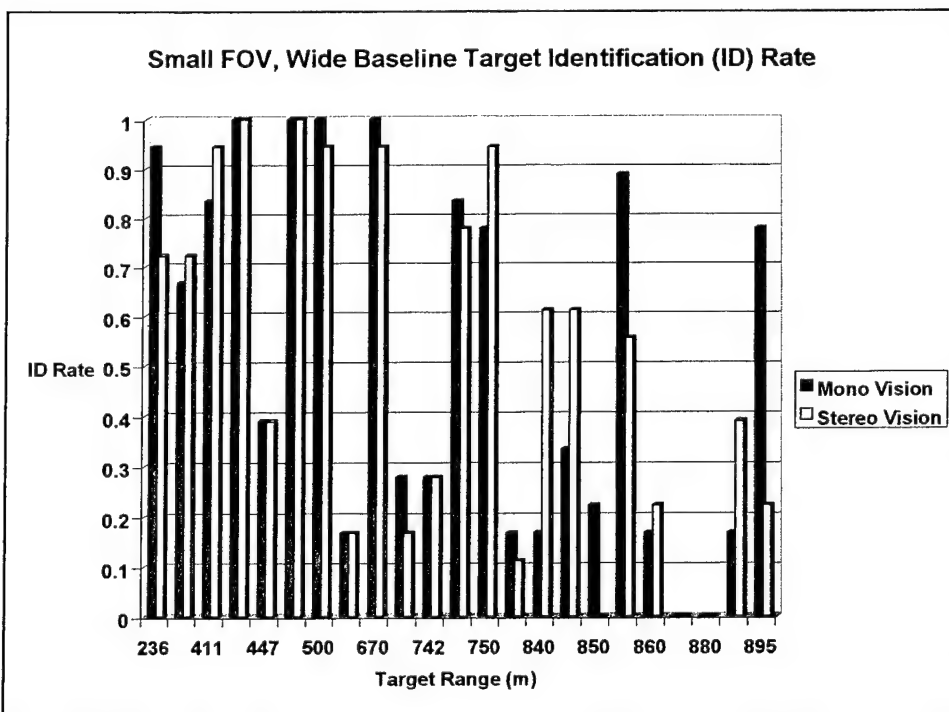


Figure A-36. The difference in correct target ID rate (mono vision minus stereo vision) for the small FOV scenes for both narrow and wide stereo baselines.

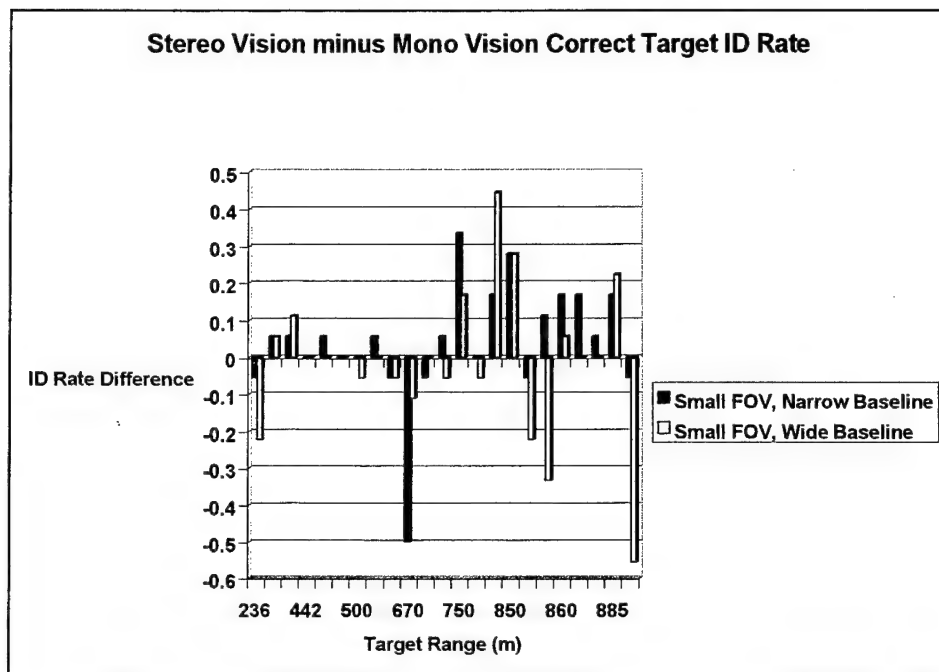


Figure A-37. Plot of observer score versus clutter rejection efficiency for the mono vision first test.

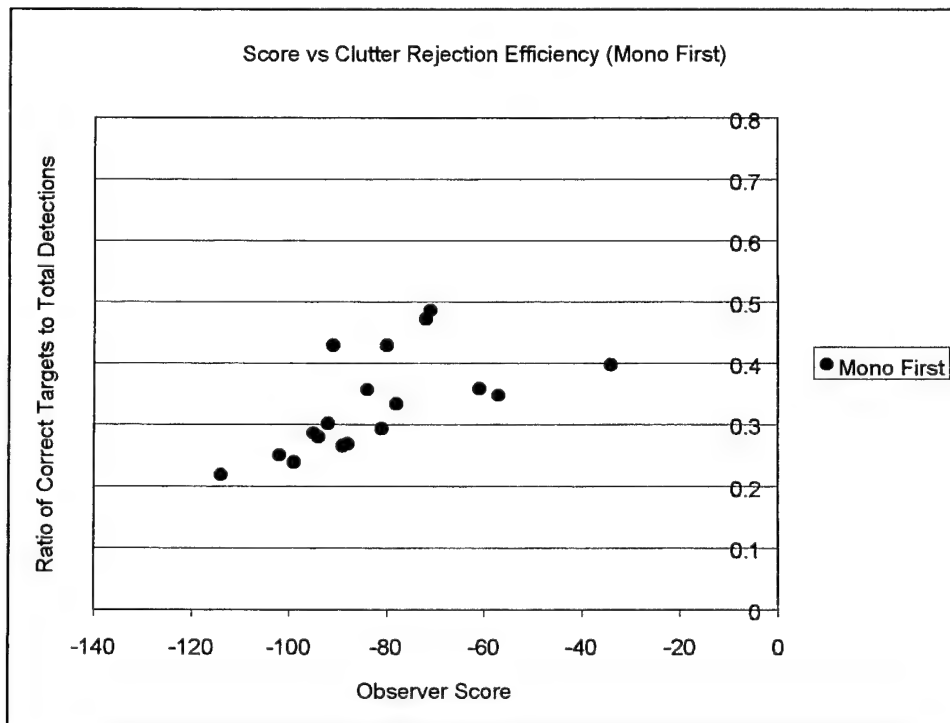


Figure A-38. Plot of observer score versus clutter rejection efficiency for the mono vision second test.

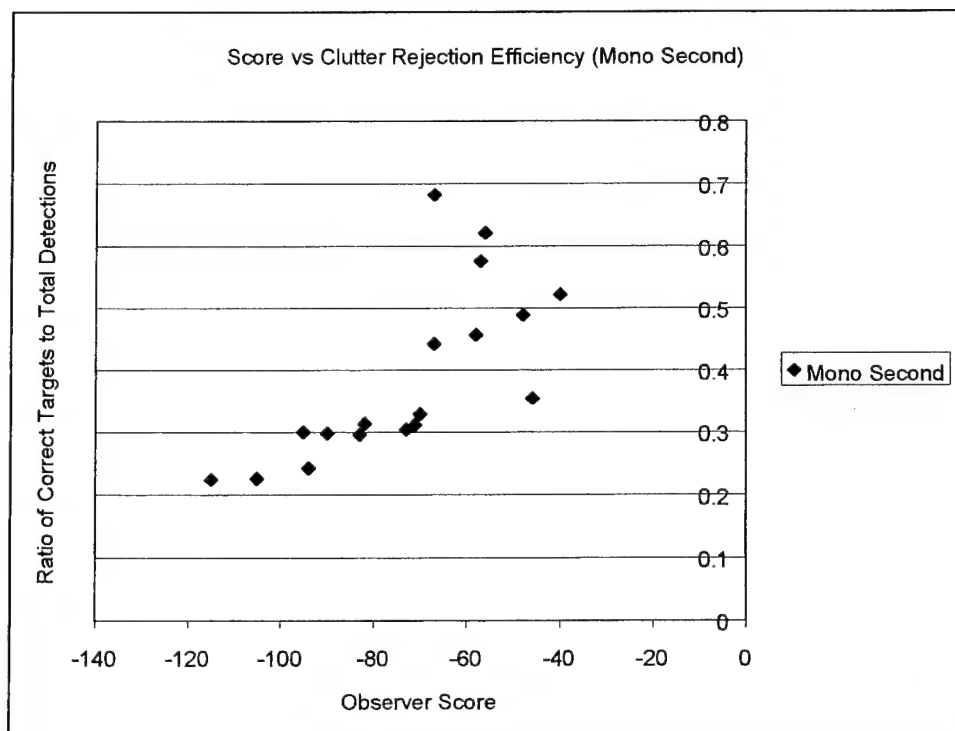


Figure A-39. Plot of observer score versus clutter rejection efficiency for the stereo vision first test.

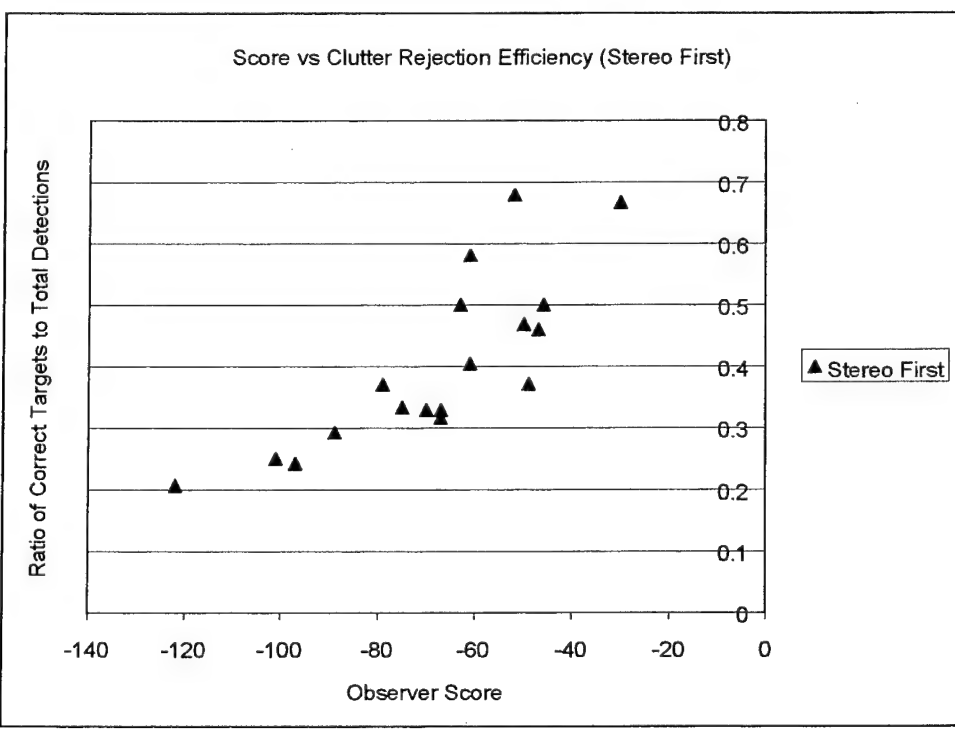


Figure A-40. Plot of observer score versus clutter rejection efficiency for the stereo vision second test.

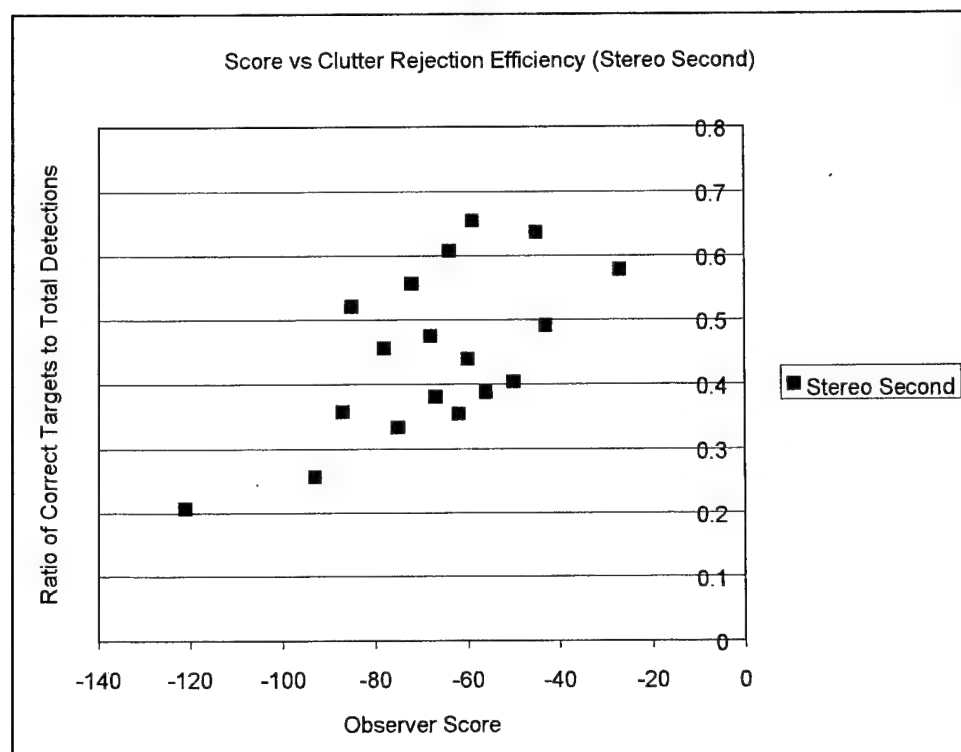


Figure A-41. Plot of observer score versus detection/clutter rejection measure for the mono vision first test.

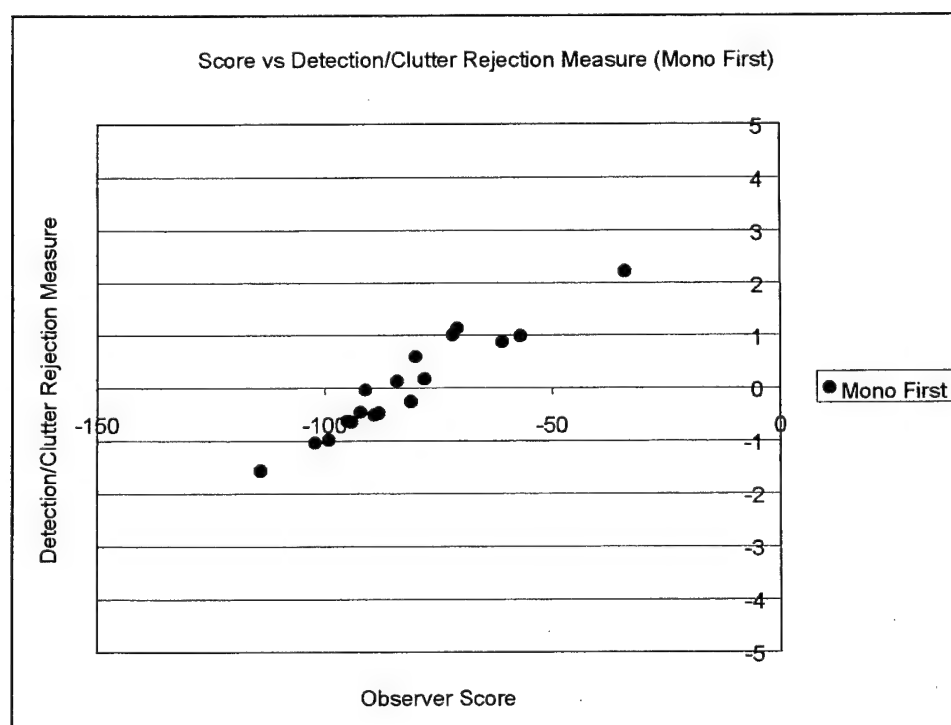


Figure A-42. Plot of observer score versus detection/clutter rejection measure for the mono vision first test.

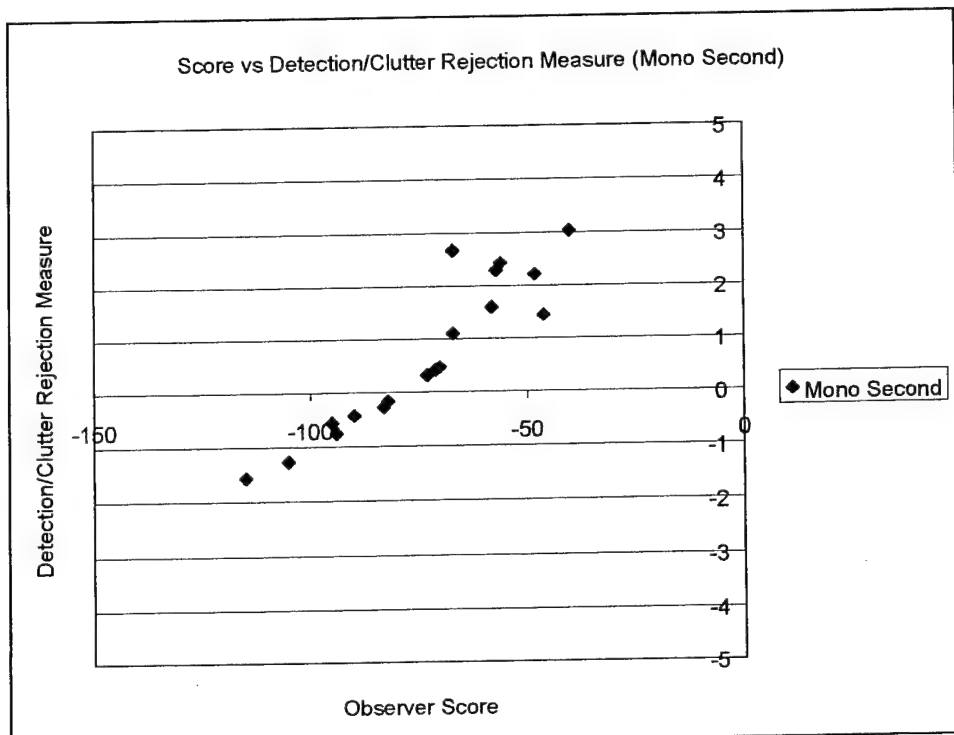


Figure A-43. Plot of observer score versus detection/clutter rejection measure for the mono vision first test.

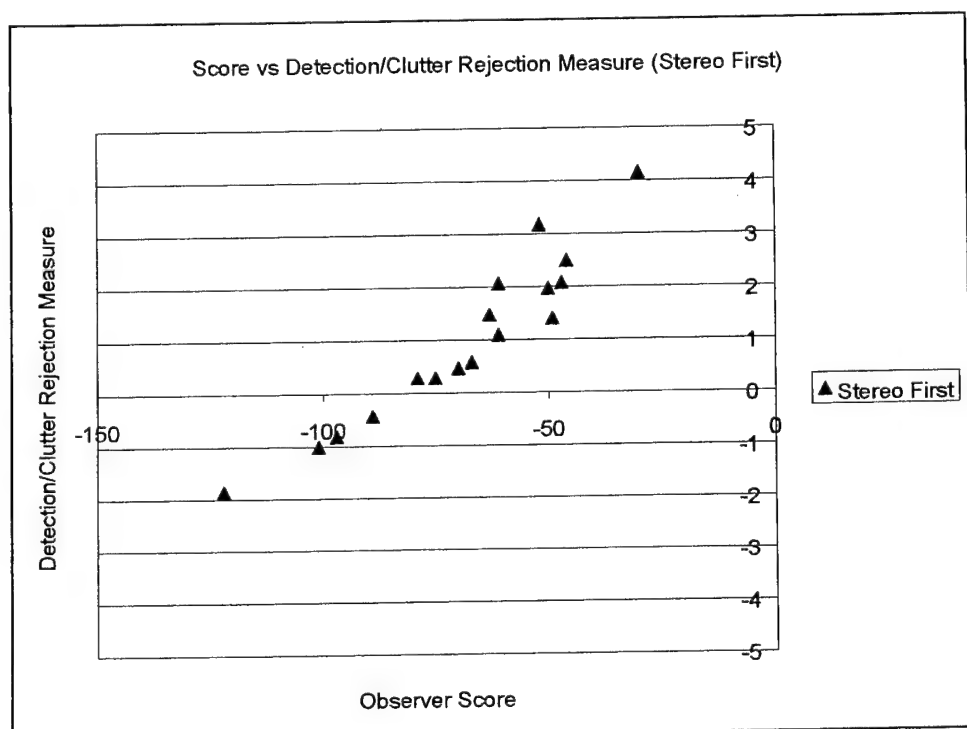


Figure A-44. Plot of observer score versus detection/clutter rejection measure for the mono vision first test.

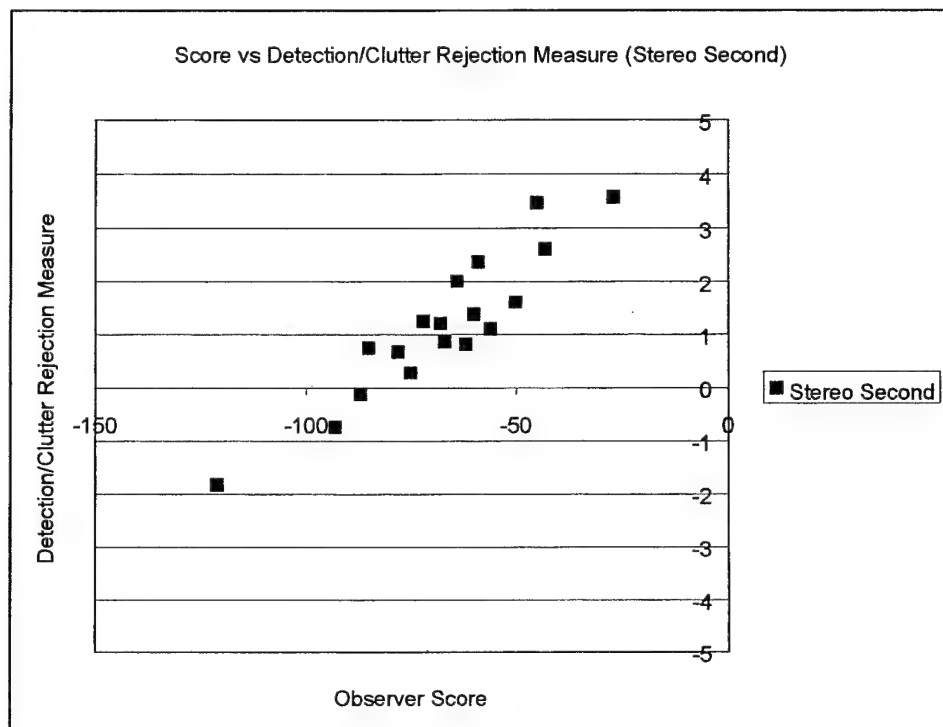


Figure a-45. Plot of observer score versus detection/clutter rejection measure for large FOV mono first test.

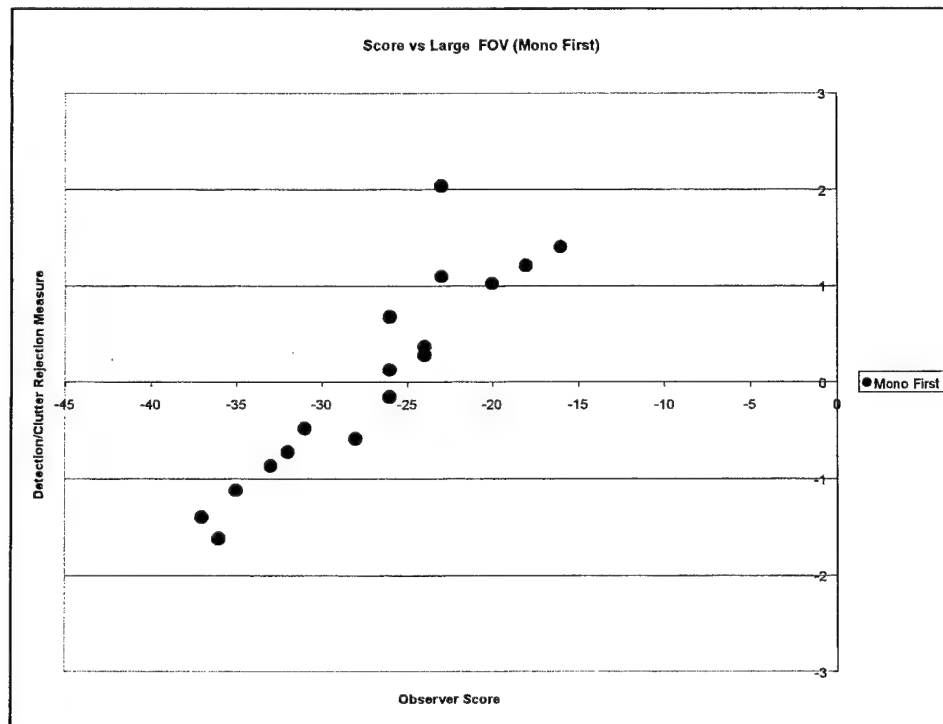


Figure A-46. Plot of observer score versus detection/clutter rejection measure for large FOV mono second test.

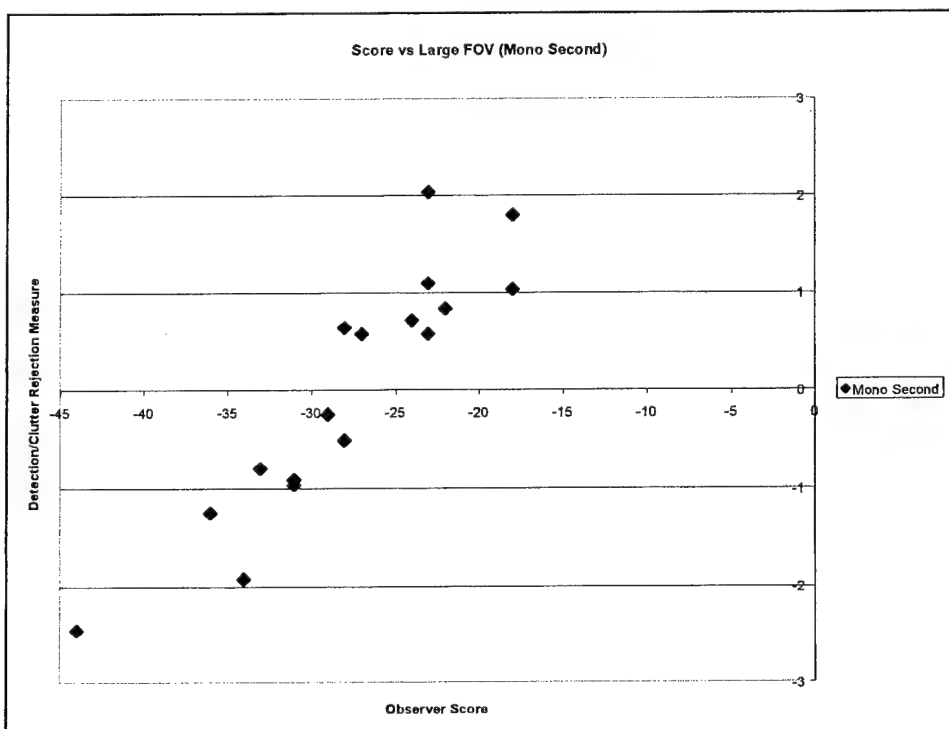


Figure A-47. Plot of observer score versus detection/clutter rejection measure for large FOV stereo first test.

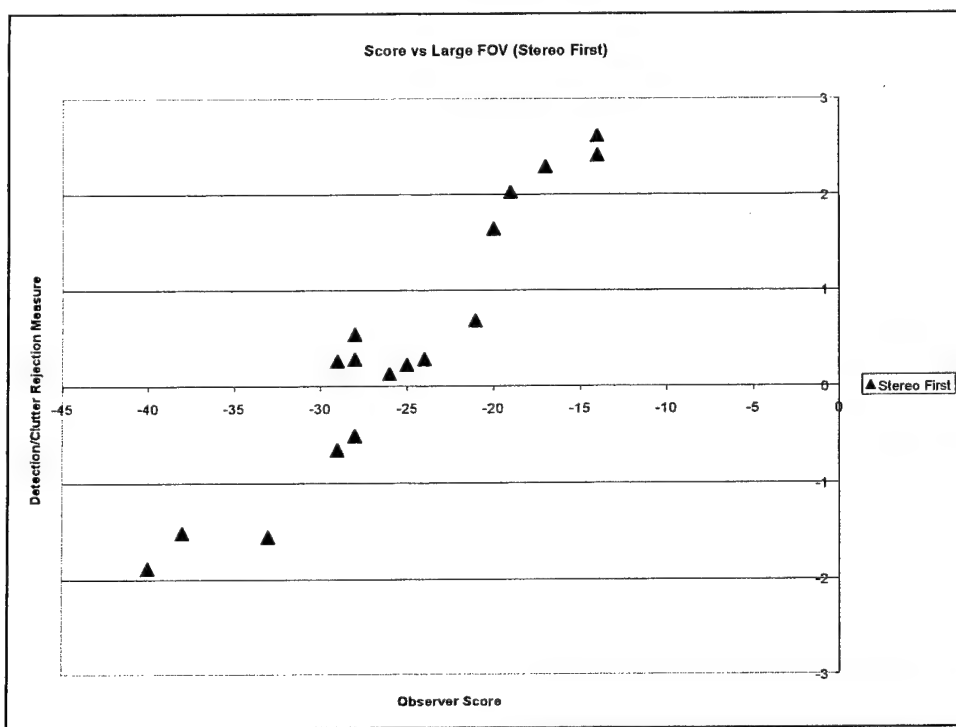


Figure A-48. Plot of observer score versus detection/clutter rejection measure for large FOV stereo second test.

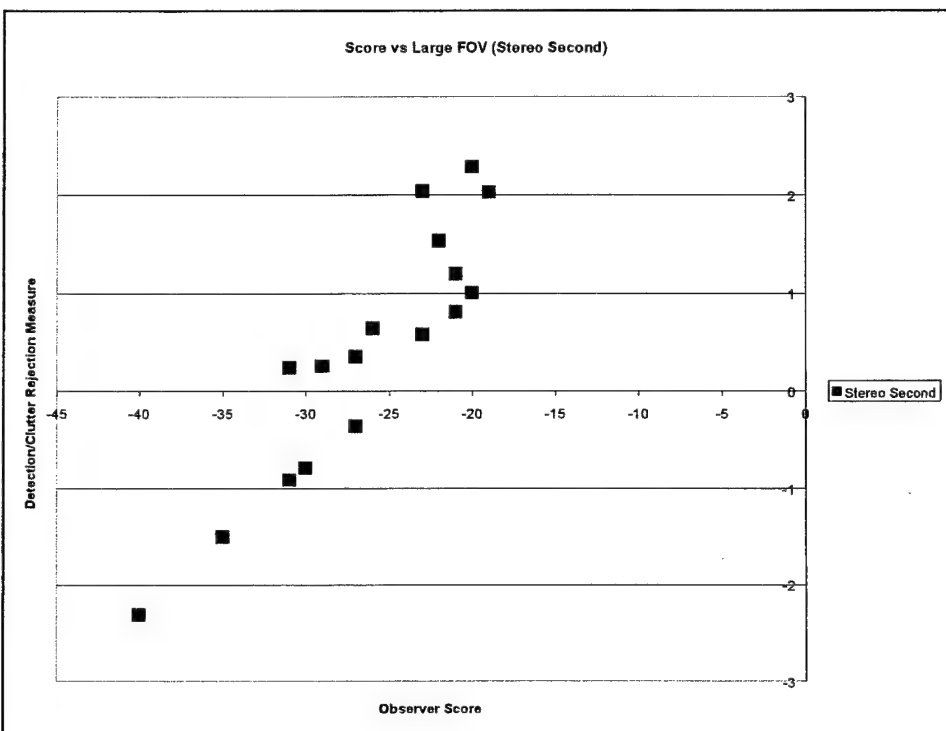


Figure A-49. Plot of ratio detection/clutter rejection measure for other orderings to that of mono first test for large FOV.

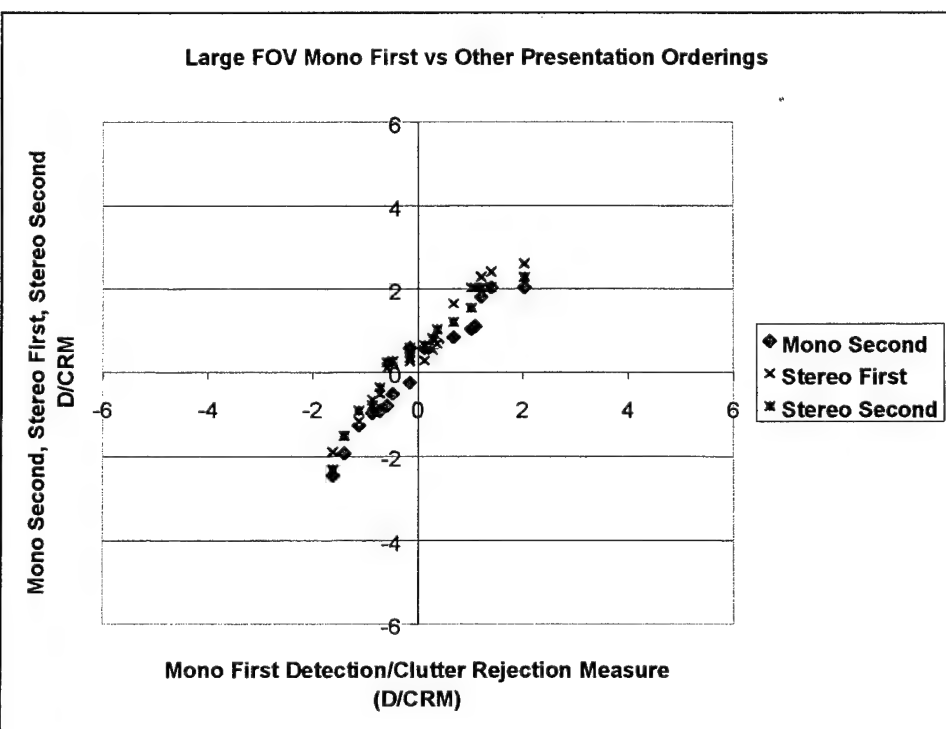


Figure A-50. Plot of ratio detection/clutter rejection measure for other orderings to that of mono first test for large FOV.

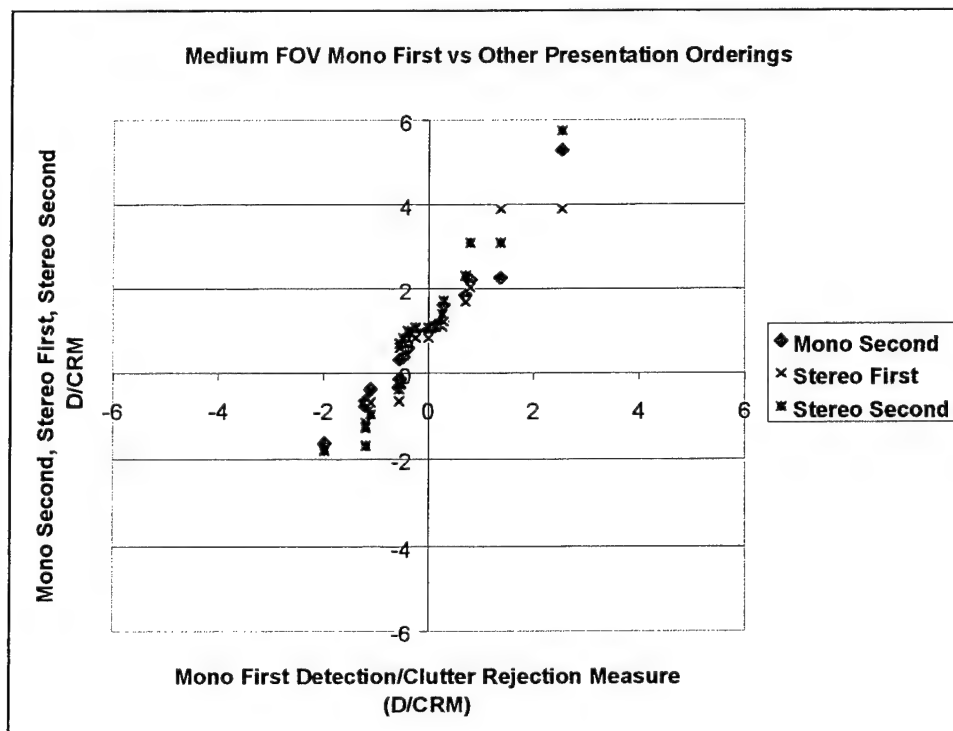


Figure A-51. Plot of ratio detection/clutter rejection measure for other orderings to that of mono first test for large FOV.

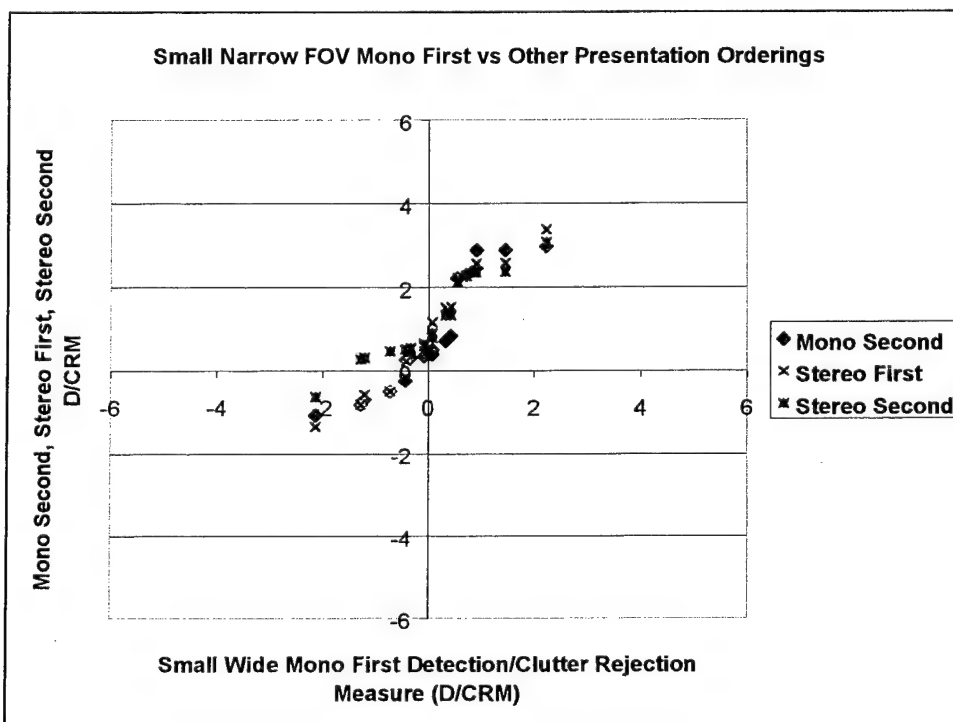


Figure A-52. Plot of ratio detection/clutter rejection measure for other orderings to that of mono first test for large FOV.

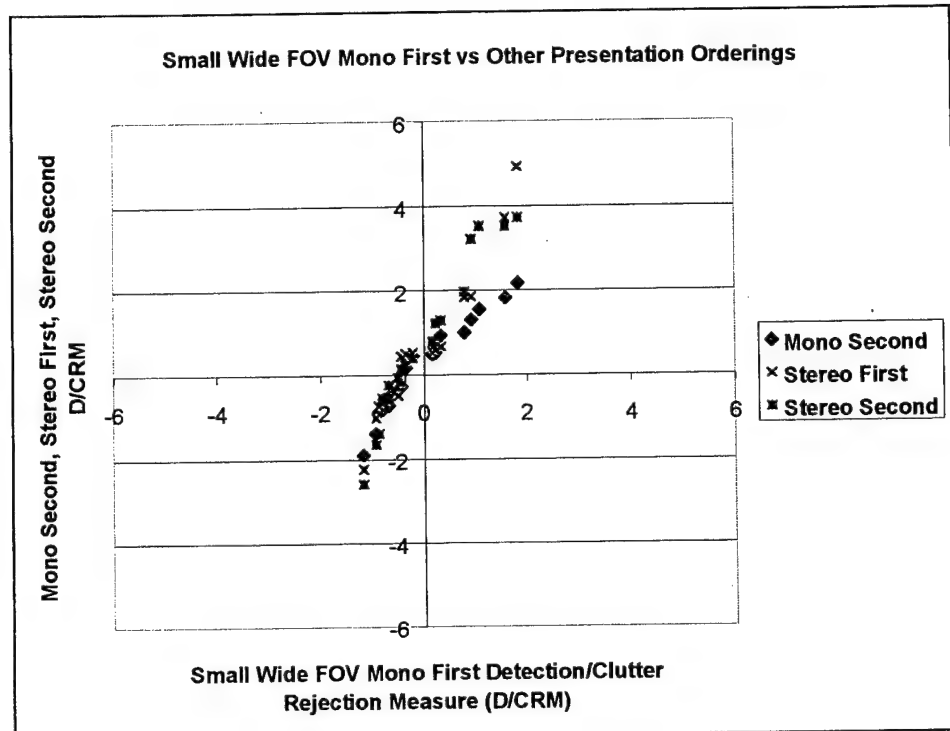


Figure A-53. Plot of ratio detection/clutter rejection measure for other orderings to that of mono first test for large FOV.

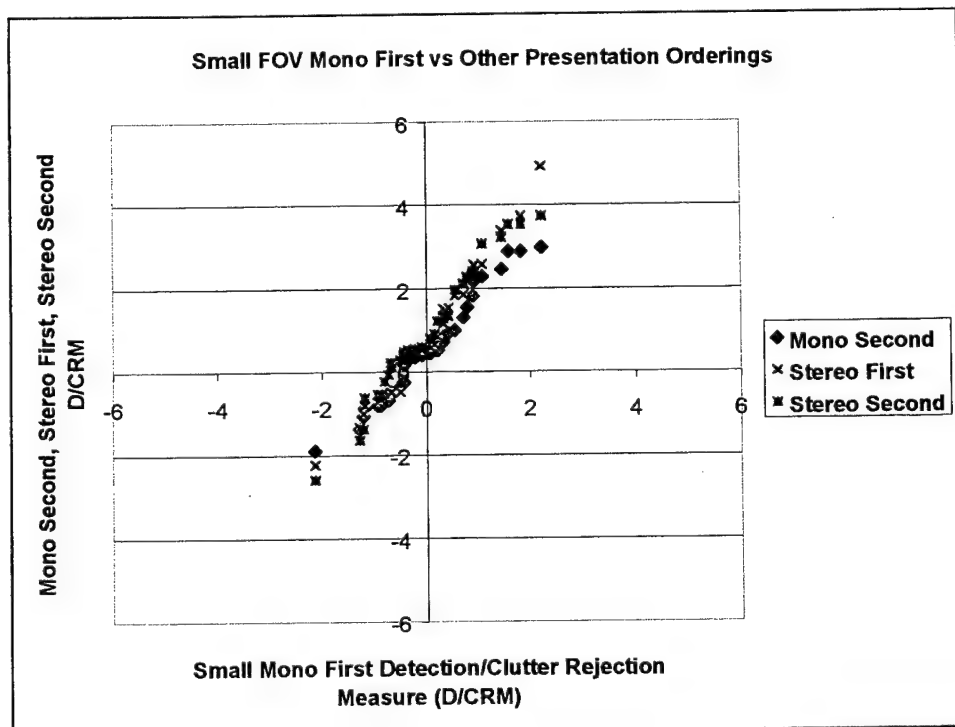


Figure A-54. Plot of mono vision versus stereo vision false alarms for the small FOV cases.

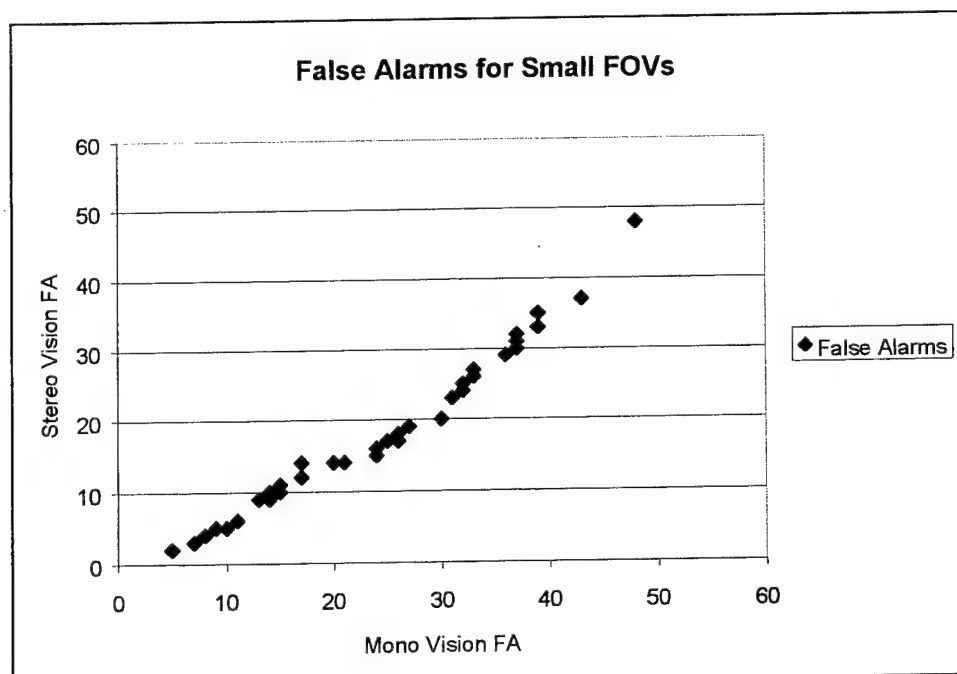
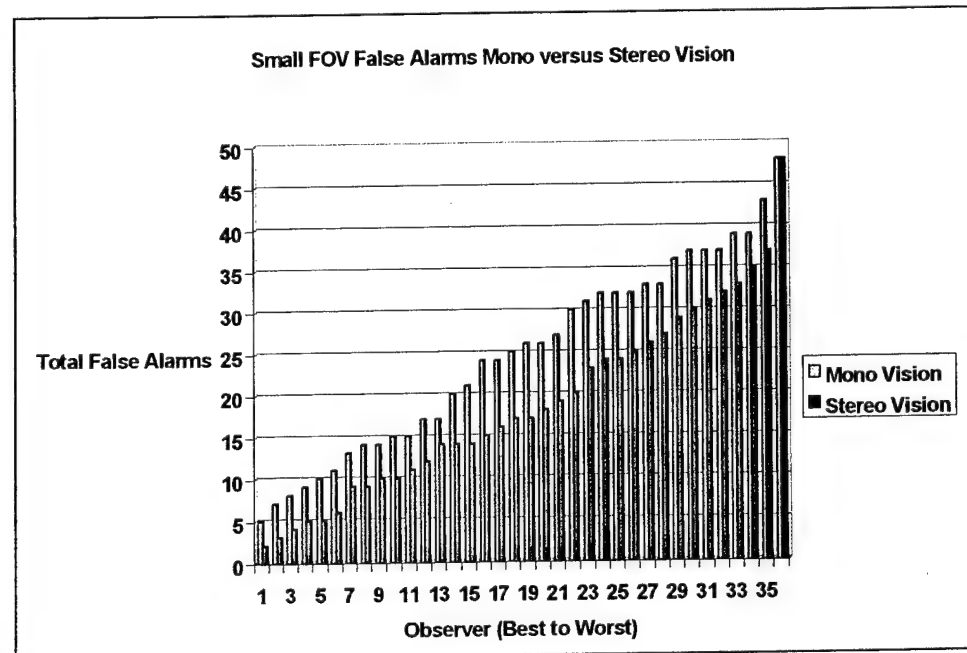


Figure A-55.
Comparison of the false target detections or false alarms for mono vision versus stereo vision for the small FOV scenes for both narrow and wide stereo baselines.



Distribution

	COPIES
DEFENSE TECH INFO CTR DTIC OCA 8725 JOHN J KINGMAN RD SUITE 0944 FT BELVOIR VA 22060-6218	1
OFFICE SECY OF DEFENSE OUSD(A&T) ODDR&E(R) DR RJ TREW 3800 DEFENSE PENTAGON WASHINGTON DC 20301-3800	1
OUSD(A&T) S&T AIR WARFARE MR R MUTZELBUG RM 3E139 3090 DEFENSE PENTAGON WASHINGTON DC 20310-3090	1
OUSD(A&T)/S&T LAND WARFARE MR A VIIIU RM 3B1060 3090 DEFENSE PENTAGON WASHINGTON DC 20310-3090	1
OASD C3I MR J BUCHHEISTER RM 3D174 6000 DEFENSE PENTAGON WASHINGTON DC 20301 6000	1
UNDER SEC OF THE ARMY DUSA OR RM 2E660 102 ARMY PENTAGON WASHINGTON DC 20310-0102	1
ASST SEC ARMY ACQUISITION LOGISTICS & TECHNOLOGY SAAL ZD RM 2E673 103 ARMY PENTAGON WASHINGTON DC 20301-0103	1
ASST SEC ARMY ACQUISITION LOGISTICS & TECHNOLOGY SAAL ZP RM 2E661 103 ARMY PENTAGON WASHINGTON DC 20310-0103	1

ASST SEC ARMY ACQUISITION LOGISTICS & TECHNOLOGY SAAL ZS RM 3E448 103 ARMY PENTAGON WASHINGTON DC 20310-0103	1
OADCOPS FORCE DEV DIR DAMO FDZ RM 31522 460 ARMY PENTAGON WASHINGTON DC 2031-0460	1
HQDA ODCSPER DAPE MR (RM 2C733) 300 ARMY PENTAGON WASHINGTON DC 20301-0300	1
US MILITARY ACADEMY MATH SCI CTR EXCELLENCE MADN MATH MAJ R HUBER THAYER HALL WEST POINT NY 10996-1786	1
US ARMY TRADOC BATTLE LAB INTEGRATION TECH & CONCEPTS DIR ATCD B FT MONROE VA 23651-5850	1
US ARMY TRADOC ANL CTR ATRC W MR A KEINTZ WSMR NM 88002-5502	1
DARPA SPECIAL PROJECTS OFFICE MR J CARLINI 3701 N FAIRFAX DR ARLINGTON VA 22203-1714	1
ARMY EVALUATION CENTER CSTE AEC MR W POLIMADEI 4120 SUSQUEHANNA AVE APG MD 21005-3013	1
ARMY EVALUATION CENTER CSTE AEC SV MR L DELATTRE 4120 SUSQUEHANNA AVE APG MD 21005-3013	1

US ARMY ARMAMENT RDEC AMSTA AR TD MR M FISSETTE BLDG 1 PICATINNY ARSENAL NJ 07806-5000	1
SBCCOM RDEC AMSSB RTD MR J ZARZYCKI 5183 BLACKHAWK RD APG MD 21010-5424	1
US ARMY MISSILE RDEC AMSMI RD DR W MCCORKLE RSA AL 35898-5240	1
NATICK SOLDIER CENTER SBCN T MR P BRANDLER KANSAS STREET NATICK MA 01760-5056	1
US ARMY TANK AUTOMTV RDEC AMSTA TR MR J CHAPIN WARREN MI 48397-5000	1
US AMRY INFO SYS ENGRG CMD AMSEL IE TD DR F JENIA FT HUACHUCA AZ 85613-5300	1
US ARMY SIM TRNG INST CMD AMSTI CG DR M MACEDONIA 12350 RESEARCH PARKWAY ORLANDO FL 32826-3726	1
US ARMY DEV TEST CMD CSTE DTC TT T APG MD 21005-5055	1
DIRECTOR US ARMY RESEACH OFFICE 4300 S MIAMI BLVD RESEARCH TRIANGLE PARK NC 27709	1
US ARMY RESEARCH LAB AMSRL D DR D SMITH 2800 POWDER MILL RD ADEPHI MD 20783-1197	1

US ARMY RESEARCH LAB AMSRL SL DR J WADE APG MD 21005-5068	1
US ARMY RESEARCH LAB AMSRL SL MR J BEILFUSS APG MD 21005-5068	1
US ARMY RESEARCH LAB AMSRL SL E DR M STARKS APG MD 21005-5068	1
US ARMY RESEARCH LAB AMSRL SL EC MR E PANUSKA APG MD 21005-5068	1
US ARMY RESEARCH LAB AMSRL SL EM DR J FEENEY APG MD 21005-5068	1
US ARMY RESEARCH LAB AMSRL SL B MS J SMITH APG MD 21005-5068	1
US ARMY RESEARCH LAB AMSRL SL B MR J FRANZ APG MD 21005-5068	1
US ARMY RESEARCH LAB AMSRL SL B MS W WINNER APG MD 21005-5068	1
US ARMY RESEARCH LAB AMSRL SL BA MS M RITONDO APG MD 21005-5068	1
US ARMY RESEARCH LAB AMSRL SL BD MR J MORRISSEY APG MD 21005-5068	1

US ARMY RESEARCH LAB AMSRSL SL BE MR D BELY APG MD 21005-5068	1
US ARMY RESEARCH LAB AMSRSL SL BN MR D FARENWALD APG MD 21005-5423	1
US ARMY RESEARCH LAB AMSRSL SL MR C HOPPER WSMR NM 88002-5513	1
US ARMY RESEARCH LAB AMSRSL SL E MR J PALOMO WSMR NM 88002-5513	1
US ARMY RESEARCH LAB AMSRSL SL EA MR R FLORES WSMR NM 88002-5513	1
US ARMY RESEARCH LAB AMSRSL SL EI MR J NOWAK FT MONMOUTH NJ 07703-5601	1
US ARMY RESEARCH LAB AMSRSL CI AI R 2800 POWDER MILL RD ADELPHI MD 20783-1197	1
US ARMY RESEARCH LAB AMSRSL CI AP 2800 POWDER MILL RD ADELPHI MD 20783-1197	3
US ARMY RESEARCH LAB AMSRSL CI LL 2800 POWDER MILL RD ADELPHI MD 20783-1197	3
US ARMY RESEARCH LAB AMSRSL CI LP BLDG 305 APG MD 21005-5068	2
US ARMY RESEARCH LAB AMSRSL SL EM ATTN J THOMPSON WSMR NM 88002-5501	1

US ARMY RESEARCH LAB AMSR IS ES ATTN P GILLESPIE ADELPHI MD 20783-1197	2
US ARMY RESEARCH LAB AMSR IS EW ATTN D TOFSTED WSMR NM 88002-5501	1
US ARMY RESEARCH LAB AMSR IS EW ATTN R SHIRKEY WSMR NM 88002-5501	1
US ARMY RESEARCH LAB AMSR HR SD ATTN V GRAYSON CUQLOCK-KNOPP APG MD 21005-5067	2
US ARMY RESEARCH LAB AMSR SL EA ATTN WR WATKINS WSMR NM 88002-5013	20
Record Copy	1
TOTAL	80